Copyright © 1984 Academic Press. Reprinted, with permission, from Infrared and Millimeter Waves, Vol. 11, pp. 239-289, 1984.

CHAPTER 7

Phase Noise and AM Noise Measurements in the Frequency Domain

Algie L. Lance, Wendell D. Seal, and Frederik Labaar

TRW Operations and Support Group
One Space Park
Redondo Beach, California

I. Introduction

Frequency sources contain noise that appears to be a superposition of causally generated signals and random, nondeterministic noises. The random noises include thermal noise, shot noise, and noises of undetermined origin (such as flicker noise). The end result is time-dependent phase and amplitude fluctuations. Measurements of these fluctuations characterize the frequency source in terms of amplitude modulation (AM) and phase modulation (PM) noise (frequency stability).

Copyright © 1984 by Academic Press, Inc.
All rights of reproduction in any form reserved.
ISBN 0-12-147711-8

The term *frequency stability* encompasses the concepts of random noise, intended and incidental modulation, and any other fluctuations of the output frequency of a device. In general, frequency stability is the degree to which an oscillating source produces the same frequency value throughout a specified period of time. It is implicit in this general definition of frequency stability that the stability of a given frequency decreases if anything except a perfect sine function is the signal wave shape.

Phase noise is the term most widely used to describe the characteristic randomness of frequency stability. The term *spectral purity* refers to the ratio of signal power to phase-noise sideband power. Measurements of phase noise and AM noise are performed in the *frequency domain* using a spectrum analyzer that provides a *frequency window* following the detector (double-balanced mixer). Frequency stability can also be measured in the *time domain* with a gated counter that provides a *time window* following the detector.

Long-term stability is usually expressed in terms of parts per million per hour, day, week, month, or year. This stability represents phenomena caused by the aging process of circuit elements and of the material used in the frequency-determining element. Short-term stability relates to frequency changes of less than a few seconds duration about the nominal frequency.

Automated measurement systems have been developed for measuring the combined phase noise of two signal sources (the two-oscillator technique) and a single signal source (the single-oscillator technique), as reported by Lance *et al.* (1977) and Seal and Lance (1981). When two source signals are applied in quadrature to a phase-sensitive detector (double-balanced mixer), the voltage fluctuations analogous to *phase fluctuations* are measured at the detector output. The single-oscillator measurement system is usually designed using a frequency cavity or a delay line as an FM discriminator. Voltage fluctuations analogous to *frequency fluctuations* are measured at the detector output.

The integrated phase noise can be calculated for any selected range of Fourier frequencies. A representation of fluctuations in the frequency domain is called *spectral density* graph. This graph is the distribution of power variance versus frequency.

II. Fundamental Concepts

In this presentation we shall attempt to conform to the definitions, symbols, and terminology set forth by Barnes *et al.* (1970). The Greek letter ν represents frequency for carrier-related measures. Modulation-related frequencies are designated f. If the carrier is considered as dc, the frequencies measured with respect to the carrier are referred to as baseband, offset from the carrier, modulation, noise, or Fourier frequencies.

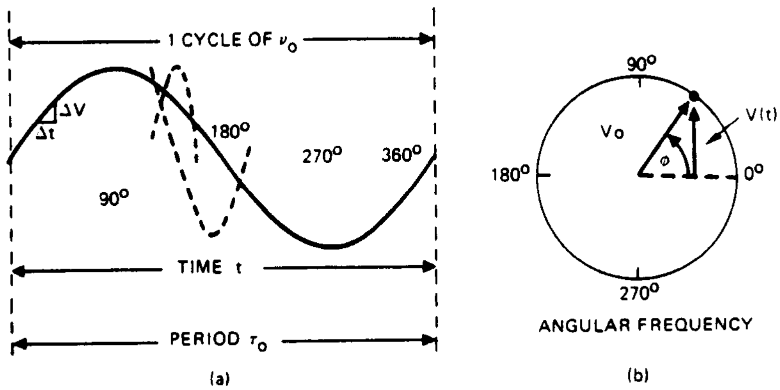

FIG. 1 Sine wave characteristics: (a) voltage V changes with time τ as (b) amplitude changes with phase angle ϕ.

A sine wave generator produces a voltage that changes in time t as the amplitude V changes with the phase angle ϕ, shown in Fig. 1. Phase is measured from a zero crossing, as illustrated by plotting the phase angle as the radius vector rotates at a constant angular rate determined by the frequency. The ideal (perfect) sine-wave-related parameters are as follows: ν_0, average (nominal) frequency of the signal; $\nu(t)$, instantaneous frequency of a signal

$$\nu(t) = \frac{1}{2\pi}\frac{d\phi}{dt}(t); \tag{1}$$

V_0, nominal peak amplitude of a signal source output; τ, period of an oscillation $(1/\nu_0)$; Ω, signal (carrier) angular frequency (rate of change of phase with time) in radians

$$\Omega = 2\pi\nu_0; \tag{2}$$

Ωt, instantaneous angular frequency; $V(t)$, instantaneous output voltage of a signal. For the ideal sine wave signal of Fig. 1, in volts,

$$V(t) = V_0 \sin(2\pi\nu_0 t). \tag{3}$$

The basic relationship between phase ϕ, frequency ν_0, and time interval τ of the ideal sine wave is given in radians by the following:

$$\phi = 2\pi\nu_0\tau, \tag{4}$$

where $\phi(t)$ is the instantaneous phase of the signal voltage, $V(t)$, defined for the ideal sine wave in radians as

$$\phi(t) = 2\pi\nu_0 t. \tag{5}$$

The instantaneous phase $\phi(t)$ of $V(t)$ for the noisy signal is

$$\phi(t) = 2\pi\nu_0 t + \phi(t), \tag{6}$$

where $\phi(t)$ is the instantaneous phase fluctuation about the ideal phase $2\pi\nu_0\tau$ of Eq. (4).

The simplified illustration in Fig. 1 shows the sine-wave signal perturbed for a short instant by noise. In the perturbed area, the Δv and Δt relationships correspond to other frequencies, as shown by the dashed-line waveforms. In this sense, frequency variations (phase noise) occur for a given instant within the cycle.

The instantaneous output voltage $V(t)$ of a signal generator or oscillator is now

$$V(t) = [V_0 + \varepsilon(t)] \sin[2\pi\nu_0 t + \phi(t)], \tag{7}$$

where V_0 and ν_0 are the nominal amplitude and frequency, respectively, and $\varepsilon(t)$ and $\phi(t)$ are the instantaneous amplitude and phase fluctuations of the signal.

It is assumed in Eq. (7) that

$$\varepsilon(t)/V_0 \ll 1 \quad \text{and} \quad \frac{\dot{\phi}(t)}{\nu_0} \ll 1 \qquad \text{for all} \quad (t), \dot{\phi}(t) = d\phi/dt. \tag{8}$$

Equation (7) can also be expressed as

$$V(T) = [V_0 + \delta\varepsilon(t)] \sin[2\pi\nu_0 t + \phi_0 + \delta\phi(t)], \tag{9}$$

where ϕ_0 is a constant, δ is the fluctuations operator, and $\delta\varepsilon(t)$ and $\delta\phi(t)$ represent the fluctuations of signal amplitude and phase, respectively.

Frequency fluctuations $\delta\nu$ are related to phase fluctuations $\delta\phi$, in hertz, by

$$\delta\nu = \frac{\delta\Omega}{2\pi} = \frac{1}{2\pi}\frac{d(\delta\phi)}{dt}, \tag{10}$$

i.e., radian frequency deviation is equal to the rate of change of phase deviation (the first-time derivative of the instantaneous phase deviation).

The fluctuations of time interval $\delta\tau$ are related to fluctuations of phase $\delta\phi$, in radians, by

$$\delta\phi = (2\pi\nu_0)\delta\tau. \tag{11}$$

In the following, y is defined as the *fractional frequency fluctuation* or fractional frequency deviation. It is the dimensionless value of $\delta\nu$ normalized to the average (nominal) signal frequency ν_0,

$$y = \delta\nu/\nu_0, \tag{12}$$

where $y(t)$ is the instantaneous fractional frequency deviation from the nominal frequency ν_0.

A. Noise Sidebands

Noise sidebands can be thought of as arising from a composite of low-frequency signals. Each of these signals modulate the carrier-producing components in both sidebands separated by the modulation frequency, as illustrated in Fig. 2. The signal is represented by a pair of symmetrical sidebands (pure AM) and a pair of antisymmetrical sidebands (pure FM).

The basis of measurement is that when noise modulation indices are small, correlation noise can be neglected. *Two signals are uncorrelated* if their phase and amplitudes have different time distributions so that they do not cancel in a phase detector. The separation of the AM and FM components are illustrated as a modulation phenomenon in Fig. 3. Amplitude fluctuations can be measured with a simple detector such as a crystal. Phase or frequency fluctuations can be detected with a discriminator. Frequency modulation (FM) noise or rms frequency deviation can also be measured with an amplitude (AM) detection system after the FM variations are converted to AM variations, as shown in Fig. 3a. The FM-AM conversion is obtained by applying two signals in phase quadrature (90°) at the inputs to a balanced mixer (detector). This is illustrated in Fig. 3 by the 90° phase advances of the carrier.

B. Spectral Density

Stability in the frequency domain is commonly specified in terms of spectral densities. There are several different, but closely related, spectral densities that are relevant to the specification and measurement of stability of the frequency, phase, period, amplitude, and power of signals. Concise, tutorial

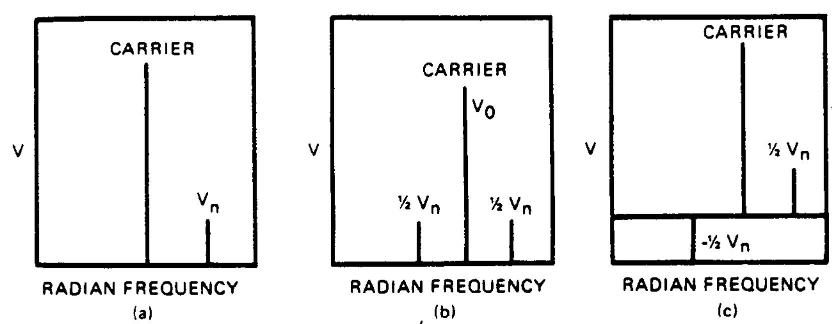

FIG. 2 (a) Carrier and single upper sideband signals; (b) symmetrical sidebands (pure AM); (c) an antisymmetrical pair of sidebands (pure FM).

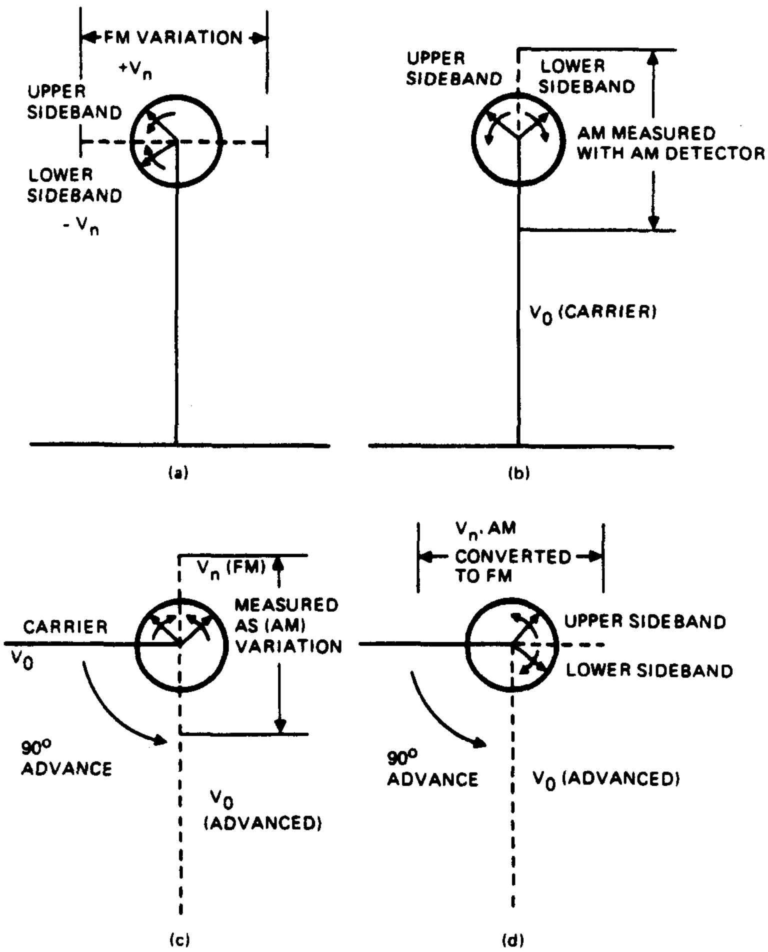

FIG. 3 (a) Relationships of the FM signal to the carrier; (b) relationship of the AM signal to the carrier; (c) carrier advanced 90° to obtain FM–AM conversion; (d) AM–FM conversion.

descriptions of twelve defined spectral densities and the relationships among them were given by Shoaf *et al.* (1973) and Halford *et al.* (1973).

Recall that in the perturbed area of the sine wave in Fig. 1 the frequencies are being produced for a given *instant of time*. This *amount of time* the signal spends in producing another frequency is referred to as the *probability density* of the generated frequencies relative to ν_0. The frequency domain plot is illustrated in Fig. 4. A graph of these probability densities over a period of time produces a continuous line and is called the *Power spectral density*.

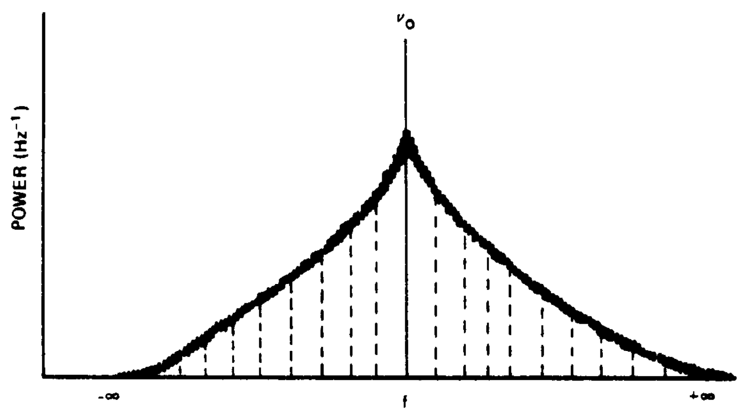

FIG. 4 A power density plot.

The spectral density is the distribution of total variance over frequency. The units of power spectral density are *power per hertz*; therefore, a plot of power spectral density obtained from amplitude (voltage) measurements requires that the voltage measurements be squared.

The spectral density of power versus frequency, shown in Fig. 4, is a *two-sided* spectral density because the range of Fourier frequencies f is from minus infinity to plus infinity.

The notation $S_g(f)$ represents the two-sided spectral density of fluctations of any specified time-dependent quantity $g(t)$. Because the frequency band is defined by the two limit frequencies of minus infinity and plus infinity, the total mean-square fluctuation of that quantity is defined by

$$G_{\text{sideband}} = \int_{-\infty}^{+\infty} S_g(f)\,df. \tag{13}$$

Two-sided spectral densities are useful mainly in pure mathematical analysis involving Fourier transformations.

Similarly, for the one-sided spectral density,

$$G_{\text{sideband}} = \int_{0}^{+\infty} S_g(f)\,df. \tag{14}$$

The two-sided and one-sided spectral densities are related as follows:

$$\int_{-\infty}^{+\infty} S_{g_2}\,df = 2\int_{0}^{+\infty} S_{g_2}\,df = \int_{0}^{+\infty} S_{g_1}\,df, \tag{15}$$

where g_1 indicates one-sided and g_2 two-sided spectral densities. It is noted that the one-sided density is twice as large as the corresponding two-sided spectral density. The terminology for single-sideband versus double-sideband signals is tòtally distinct from the one-sided spectral density versus two-sided spectral terminology. They are totally different concepts. The definitions and concepts of spectral density are set forth in NBS Technical Note 632 (Shoaf *et al.*, 1973).

C. Spectral Densities of Phase Fluctuations in the Frequency Domain *

The spectral density $S_y(f)$ of the instantaneous fractional frequency fluctuations $y(t)$ is defined as a measure of frequency stability, as set forth by Barnes *et al.* (1970). $S_y(f)$ is the one-sided spectral density of *frequency fluctuations* on a "per hertz" basis, i.e., the dimensionality is Hz^{-1}. The range of Fourier frequency f is from *zero to infinity*. $S_{\delta\nu}(f)$, in hertz squared per hertz, is the spectral density of *frequency fluctuations* $\delta\nu$. It is calculated as

$$S_{\delta\nu}(f) = \frac{(\delta\nu_{\mathrm{rms}})^2}{\text{bandwidth used in the measurement of } \delta\nu_{\mathrm{rms}}}. \tag{16}$$

The range of the Fourier frequency f is from *zero to infinity*.

The spectral density of *phase fluctuations* is a normalized frequency domain measure of phase fluctuation sidebands. $S_{\delta\phi}(f)$, in radians squared per hertz, is the one-sided spectral density of the phase fluctuations on a "per hertz" basis:

$$S_{\delta\phi}(f) = \frac{\delta\phi_{\mathrm{rms}}}{\text{bandwidth used in the measurement of } \delta\phi_{\mathrm{rms}}}. \tag{17}$$

The power spectral densities of phase and frequency fluctuation are related by

$$S_{\delta\phi}(f) = (\nu_0^2/f)S_y(f). \tag{18}$$

The range of the Fourier frequency f is from *zero to infinity*.

$S_{\delta\Omega}(f)$, in radians squared Hertz squared per hertz is the spectral density of angular frequency fluctuations $\delta\Omega$:

$$S_{\delta\Omega}(f) = (2\pi)^2 S_{\delta\nu}(f). \tag{19}$$

The defined spectral densities have the following relationships:

$$S_{\delta\nu}(f) = \nu_0^2 S_y(f) = (1/2\pi)^2 S_{\delta\Omega}(f) = f^2 S_{\delta\phi}(f); \tag{20}$$

$$S_{\delta\phi}(f) = (1/\omega)^2 S_{\delta\Omega}(f) = (\nu_0/f)^2 S_y(f) = [S_{\delta\nu}(f)/f^2]. \tag{21}$$

Note that Eq. (20) is hertz squared per hertz, whereas Eq. (21) is in radians squared per hertz.

The term $S_{\sqrt{rf P}}(\nu)$, in watts per hertz, is the spectral density of the (square

* See Appendix Note # 30

root of) radio frequency power P. The power of a signal is dispersed over the frequency spectrum owing to noise, instability, and modulation. This concept is similar to the concept of spectral density of voltage fluctuations $S_{\delta v}(f)$. Typically, $S_{\delta v}(f)$ is more convenient for characterizing a baseband signal where voltage, rather than power, is relevant. $S_{\sqrt{\mathrm{rf}P}}(\nu)$ is typically more convenient for characterizing the dispersion of the signal power in the vicinity of the nominal carrier frequency ν_0. To relate the two spectral densities, it is necessary to specify the impedance associated with the signal.

A definition of frequency stability that relates the actual sideband power of phase fluctuations with respect to the carrier power level, discussed by Glaze (1970), is called $\mathscr{L}(f)$. For a signal with PM and with no AM, $\mathscr{L}(f)$ is the normalized version of $S_{\sqrt{\mathrm{rf}P}}(\nu)$, with its frequency parameter f referenced to the signal's average frequency ν_0 as the origin such that f equals $\nu - \nu_0$. If the signal also has AM, $\mathscr{L}(f)$ is the normalized version of those portions of $S_{\sqrt{\mathrm{rf}P}}(\nu)$ that are phase-modulation sidebands.

Because f is the Fourier frequency difference $(\nu - \nu_0)$, the range of f is from minus ν_0 to plus infinity. Since $\mathscr{L}(f)$ is a normalized density (phase noise sideband power),

$$\int_{-\nu_0}^{+\infty} \mathscr{L}(f)\, df = 1. \qquad (22) \quad *$$

$\mathscr{L}(f)$ is defined as the ratio of the power in one sideband, referred to the input carrier frequency on a per hertz of bandwidth spectral density basis, to the total signal power, at Fourier frequency difference f from the carrier, *per one device*. It is a normalized frequency domain measure of phase fluctuation sidebands, expressed in decibels relative to the carrier per hertz:

$$\mathscr{L}(f) = \frac{\text{power density (one phase modulation sideband)}}{\text{carrier power}}. \qquad (23)$$

For the types of signals under consideration, by definition the two phase-noise sidebands (lower sideband and upper sideband, at $-f$ and f from ν_0, respectively) of a signal are approximately coherent with each other, and they are of approximately equal intensity.

It was previously show that the measurement of phase fluctuations (phase noise) required driving a double-balanced mixer with two signals in phase quadrature so the FM–AM conversion resulted in voltage fluctuations at the mixer output that were analogous to the phase fluctuations. The operation of the mixer when it is driven at quadrature is such that the amplitudes of the two phase sidebands are added linearly in the output of the mixer, resulting in four times as much power in the output as would be present if only one of the phase sidebands were allowed to contribute to the output

* See Appendix Note # 31

of the mixer. Hence, for $|f| < \nu_0$, and considering only the phase modulation portion of the spectral density of the (square root of) power, we obtain

$$S_{\delta V}(|f|)/(V_{\mathrm{rms}})^2 \cong 4[S_{\sqrt{\mathrm{rf}P}}(\nu_0 + f)]/(P_{\mathrm{tot}}) \tag{24}$$

and, using the definition of $\mathscr{L}(f)$,

$$\mathscr{L}(f) \equiv [S_{\sqrt{\mathrm{rf}P}}(\nu_0 + f)]/(P_{\mathrm{tot}}) \cong \tfrac{1}{2}S_{\delta\phi}(|f|). \tag{25}$$

Therefore, for the condition that the phase fluctuations occurring at rates (f) and faster are small compared to one radian, a good approximation in radians squared per hertz for one unit is

$$\mathscr{L}(f) = \tfrac{1}{2}S_{\delta\phi}(f). \tag{26}$$

If the small angle condition is not met, Bessel-function algebra must be used to relate $\mathscr{L}(f)$ to $S_{\delta\phi}(f)$.

The NBS-defined spectral density is usually expressed in decibels relative to the carrier per hertz and is calculated for one unit as

$$\mathscr{L}(f) = 10\log[\tfrac{1}{2}S_{\delta\phi}(f)]. \tag{27}$$

It is very important to note that the theory, definitions, and equations previously set forth relate to a single device.

D. Modulation Theory and Spectral Density Relationships

Applying a sinusoidal frequency modulation f_m to a sinusoidal carrier frequency ν_0 produces a wave that is sinusoidally advanced and retarded in phase as a function of times. The instantaneous voltage is expressed as,

$$V(t) = V_0 \sin(2\pi\nu_0 t + \Delta\phi \sin 2\pi f_m t), \tag{28}$$

where $\Delta\phi$ is the *peak phase deviation* caused by the modulation signal.

The first term inside the parentheses represents the linearly progressing phase of the carrier. The second term is the phase variation (advancing and retarded) from the linearly progressing wave. The effects of modulation can be expressed as *residual f_m noise* or as *single-sideband phase noise*. For modulation by a single sinusoidal signal, the peak-frequency deviation of the carrier (ν_0) is

$$\Delta\nu_0 = \Delta\phi \cdot f_m, \tag{29}$$

$$\Delta\phi = \Delta\nu_0/f_m, \tag{30}$$

where f_m is the modulation frequency. This ratio of peak frequency deviation to modulation frequency is called *modulation index m* so that $\Delta\phi = m$ and

$$m = \Delta\nu_0/f_m. \tag{31}$$

The frequency spectrum of the modulated carrier contains frequency components (sidebands) other than the carrier. For small values of modulation index ($m \ll 1$), as is the case with random phase noise, only the carrier and first upper and lower sidebands are significantly high in energy. The ratio of the amplitude of either single sideband to the amplitude of the carrier is

$$V_{sb}/V_0 = m/2. \tag{32}$$

This ratio is expressed in decibels below the carrier and is referred to as dBc for the given bandwidth B:

$$\begin{aligned} V_{sb}/V_0 &= 20 \log(m/2) = 20 \log(\Delta\nu_0/2f_m) \\ &= 10 \log(m/2)^2 = 10 \log(\Delta\nu_0/2f_m)^2. \end{aligned} \tag{33}$$

If the frequency deviation is given in terms of its rms value, then

$$\Delta\nu_{rms} = \Delta\nu_0/\sqrt{2}. \tag{34}$$

Equation (33) now becomes

$$\begin{aligned} V_{sb}/V_0 = \mathscr{L}(f) &= 20 \log(\Delta\nu_{rms}/\sqrt{2}f_m) \\ &= 10 \log(\Delta\nu_{rms}/\sqrt{2}f_m)^2. \end{aligned} \tag{35}$$

The ratio of single sideband to carrier power in decibels (carrier) per hertz is

$$\mathscr{L}(f) = 20 \log(\Delta\nu_{rms}/f_m) - 3 \tag{36}$$

and, in decibels relative to one squared radian per hertz,

$$S_{\delta\phi}(f) = 20 \log(\Delta\nu_{rms}/f_m). \tag{37}$$

The interrelationships of modulation index, peak frequency deviation, rms frequency, and spectral density of phase fluctuations can be found from the following:

$$\tfrac{1}{2}m = \Delta\nu_0/2f_m = \Delta\nu_{rms}/\sqrt{2}f_m, \tag{38}$$

$$= 10 \exp(\mathscr{L}(f)/10) = \tfrac{1}{2}S_{\delta\phi}(f); \tag{39}$$

or

$$\tfrac{1}{2}m = \Delta\nu_{rms}/\sqrt{2}f_m = \sqrt{10 \exp(\mathscr{L}(f)/10)} = \sqrt{\tfrac{1}{2}S_{\delta\phi}(f)}, \tag{40}$$

and

$$\begin{aligned} m &= \Delta\nu_0/f_m = 2\Delta\nu_{rms}/\sqrt{2}f_m \\ &= 2\sqrt{10 \exp(\mathscr{L}(f)/10)} = 2\sqrt{\tfrac{1}{2}S_{\delta\phi}(f)}. \end{aligned} \tag{41}$$

The basic relationships are plotted in Fig. 5.

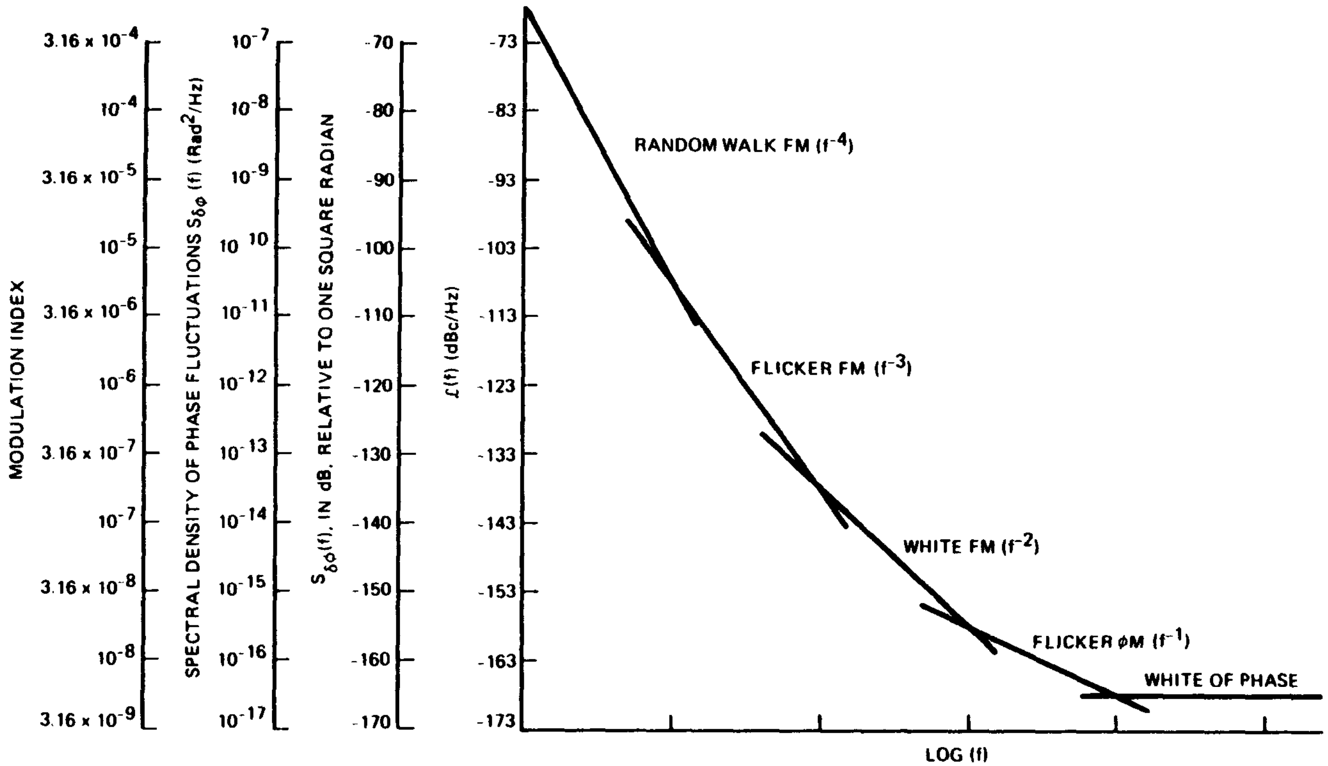

FIG. 5 Spectral density relationships.

E. Noise Processes

The spectral density plot of a typical oscillator's output is usually a combination of different noise processes. It is very useful and meaningful to categorize these processes because the first job in evaluating a spectral density plot is to determine which type of noise exists for the particular range of Fourier frequencies.

The two basic categories are the *discrete-frequency noise* and the *power-law noise* process. Discrete-frequency noise is a type of noise in which there is a dominant observable probability, i.e., deterministic in that they can usually be related to the mean frequency, power-line frequency, vibration frequencies, or ac magnetic fields, or to Fourier components of the nominal frequency. Discrete-frequency noise is illustrated in the frequency domain plot of Fig. 6. These frequencies can have their own spectral density plots, which can be defined as noise on noise.

Power-law noise processes are types of noise that produce a certain slope on the one-sided spectral density plot. They are characterized by their dependence on frequency. The spectral density plot of a typical oscillator output is usually a combination of the various power-law processes.

In general, we can classify the power-law noise processes into five categories. These five processes are illustrated in Fig. 5, which can be referred to with respect to the following description of each process.

(1) *Random walk FM* (random walk of frequency). The plot goes down as $1/f^4$. This noise is usually very close to the carrier and is difficult to measure. It is usually related to the oscillator's physical environment (mechanical shock, vibration, temperature, or other environmental effects).

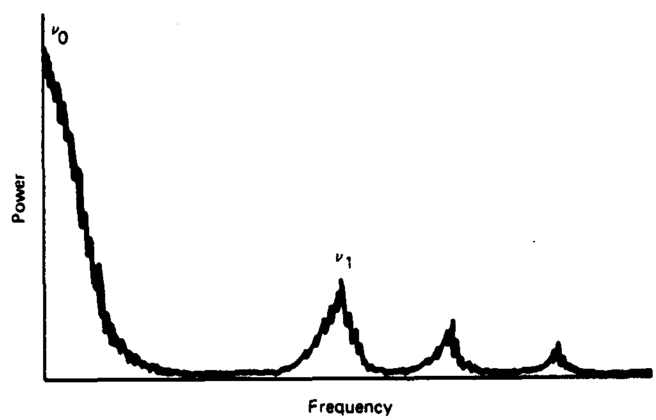

Fig. 6 A basic discrete-frequency signal display.

(2) *Flicker FM* (flicker of frequency). The plot goes down as $1/f^3$. This noise is typically related to the physical resonance mechanism of the active oscillator or the design or choice of parts used for the electronic or power supply, or even environmental properties. The time domain frequency stability over extended periods is constant. In high-quality oscillators, this noise may be marked by white FM ($1/f^2$) or flicker phase modulation ϕM ($1/f$). It may be masked by drift in low-quality oscillators.

(3) *White FM* (white frequency, random walk of phase). The plot goes down as $1/f^2$. A common type of noise found in passive-resonator frequency standards. Cesium and rubidium frequency standards have white FM noise characteristic because the oscillator (usually quartz) is locked to the resonance feature of these devices. This noise gets better as a function of time until it (usually) becomes flicker FM ($1/f^3$) noise.

(4) *Flicker ϕM* (flicker modulation of phase). The plot goes down as $1/f$. This noise may relate to the physical resonance mechanism in an oscillator. It is common in the highest-quality oscillators. This noise can be introduced by noisy electronics—amplifiers necessary to bring the signal amplitude up to a usable level—and frequency multipliers. This noise can be reduced by careful design and by hand-selecting all components.

(5) *White ϕM* (white phase). White phase noise plot is flat f^0. Broadband phase noise is generally produced in the same way as flicker ϕM ($1/f$). Late stages of amplification are usually responsible. This noise can be kept low by careful selection of components and by narrow-band filtering at the output.

The power-law processes are illustrated in Fig. 5.

F. Integrated Phase Noise

The integrated phase noise is a measure of the phase-noise contribution (rms radians, rms degrees) over a designated range of Fourier frequencies. The integration is a process of summation that must be performed on the measured spectral density within the actual IF bandwidth (B) used in the measurement of $\delta\phi_{\mathrm{rms}}$. Therefore, the spectral density $S_{\delta\phi}(f)$ must be unnormalized to the particular bandwidth used in the measurement. Define $S_u(f)$, in radians squared, as the unnormalized spectral density:

$$S_u(f) = 2[10 \exp(\mathscr{L}(f) + 10 \log B)/10]. \tag{42}$$

Then, the integrated phase noise over the band of Fourier frequencies (f_1 to f_n) *where measurements are performed using a constant IF bandwidth*, in radians squared, is

$$S_B(f_1 \text{ to } f_n) = \int_{f_1}^{f_n} S_u(f)\, df. \tag{43}$$

or, in rms radians,

$$S_B(f_1 \text{ to } f_n) = \sqrt{\sum S_u(f_1) + S_u(f_2) = \cdots = S_u(f_n)}, \tag{44}$$

and the integrated phase noise in rms degrees is calculated as

$$S_B(360/2\pi). \tag{45}$$

The integrated phase noise in decibels relative to the carrier is calculated as

$$S_B = 10\log(\tfrac{1}{2}S_B^2). \tag{46}$$

The previous calculations correspond to the illustration in Fig. 7, which includes two bandwidths (B1 and B2) over two ranges of Fourier frequencies.

In the measurement program, different IF bandwidths are used as set forth by Lance *et al.* (1977). The total integrated phase noise over the different ranges of Fourier frequencies, which are measured at constant bandwidths as illustrated, is calculated in rms radians as follows:

$$S_{B\text{tot}} = \sqrt{(S_{B1})^2 + (S_{B2})^2 + \cdots + (S_{Bn})^2}, \tag{47}$$

where it is recalled that the summation is performed in terms of radians squared.

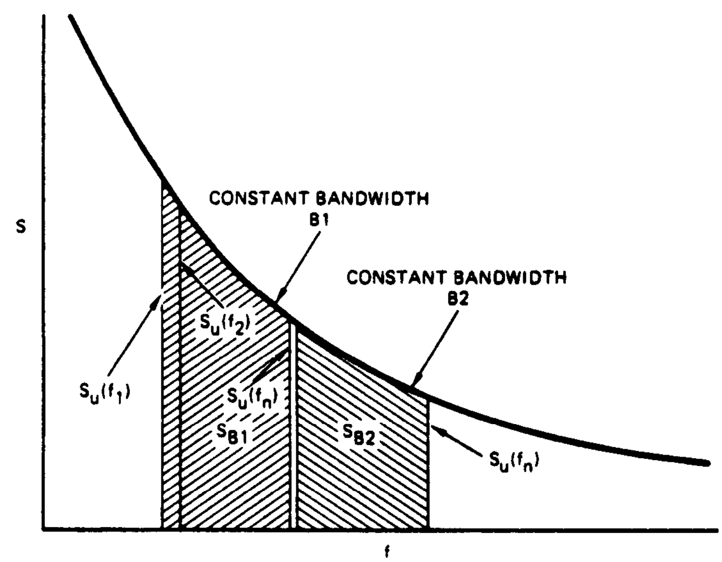

FIG. 7 Integrated phase noise over Fourier frequency ranges at which measurements were performed using constant bandwidth.

G. AM Noise in the Frequency Domain

The spectral density of AM fluctuations of a signal follows the same general derivation previously given for the spectral density of phase fluctations. Amplitude fluctuations $\delta\varepsilon$ of the signal under test produces voltage fluctuations δA at the output of the mixer. Interpretating the mean-square fluctuations $\delta\varepsilon$ and δ in spectal density fashion, we obtain $S_{\delta\varepsilon}(f)$, the spectral density of amplitude fluctuations $\delta\varepsilon$ of a signal in volts squared per hertz:

$$S_{\delta\varepsilon}(f) = (\tfrac{1}{2}V_0)^2[S_{\delta A}(f)/(A_{\mathrm{rms}})^2]. \tag{48}$$

The term $m(f)$ is the normalized version of the amplitude modulation (AM) portion of $S_{\sqrt{\mathrm{rf}\,P}}(\nu)$, with its frequency parameter f referenced to the signal's average frequency ν_0, taken as the origin such that the difference frequency f equals $\nu - \nu_0$. The range of Fourier frequency difference f is from minus ν_0 to plus infinity.

The term $m(f)$ is defined as the ratio of the spectral density of *one amplitude-modulated sideband* to the *total signal power*, at Fourier frequency difference f from the signal's average frequency ν_0, for a single specified signal or device. The dimensionality is per hertz. $\mathscr{L}(f)$ and $m(f)$ are similar functions; the former is a measure of phase-modulated (PM) sidebands, the later is a corresponding measure of amplitude-modulated (AM) sidebands. We introduce the symbol $m(f)$ to have useful terminology for the important concept of normalized AM sideband power.

For the types of signals under consideration, by definition the two amplitude-fluctuation sidebands (lower sideband and upper sideband, at $-f$ f from ν_0, respectively) of a signal are coherent with each other. Also, they are of equal intensity. The operation of the mixer when it is driven at colinear phase is such that the amplitudes of the two AM sidebands are added linearly in the output of the mixer, resulting in four times as much power in the output as would be present if only one of the AM sidebands were allowed to contribute to the output of the mixer. Hence, for $|f| < \nu_0$,

$$S_{\mathrm{A}}(|f|)/(\mathrm{A}_{\mathrm{rms}})^2 = 4[S_{\sqrt{\mathrm{rf}P}}(\nu_0 + f)]/P_{\mathrm{tot}}, \tag{49}$$

and, using the definition

$$m(f) \equiv [S_{\sqrt{\mathrm{rf}P}}(\nu_0 + f)]/P_{\mathrm{tot}}, \tag{50}$$

we find, in decibels (carrier) per hertz,

$$m(f) = (1/2V_0^2)S_{\delta\varepsilon}(|f|). \tag{51}$$

III. Phase-Noise Measurements Using the Two-Oscillator Technique *

A functional block diagram of the two-oscillator system for measuring phase noise is shown in Fig. 8. NBS has performed phase noise measurements since 1967 using this basic system. The signal level and sideband levels can be measured in terms of voltage or power. The low-pass filter prevents local oscillator leakage power from overloading the spectrum analyzer when baseband measurements are performed at the Fourier (offset) frequencies of interest. Leakage signals will interfere with autoranging and with the dynamic range of the spectrum analyzer.

The low-noise, high-gain preamplifier provides additional system sensitivity by amplyfying the noise signals to be measured. Also, because spectrum analyzers usually have high values of noise figure, this amplifier is very desirable. As an example, if the high-gain preamplifier had a noise figure of 3 dB and the spectrum analyzer had a noise figure of 18 dB, the system sensitivity at this point has been improved by 15 dB. The overall system sensitivity would not necessarily be improved 15 dB in all cases, because the limiting sensitivity could have been imposed by a noisy mixer.

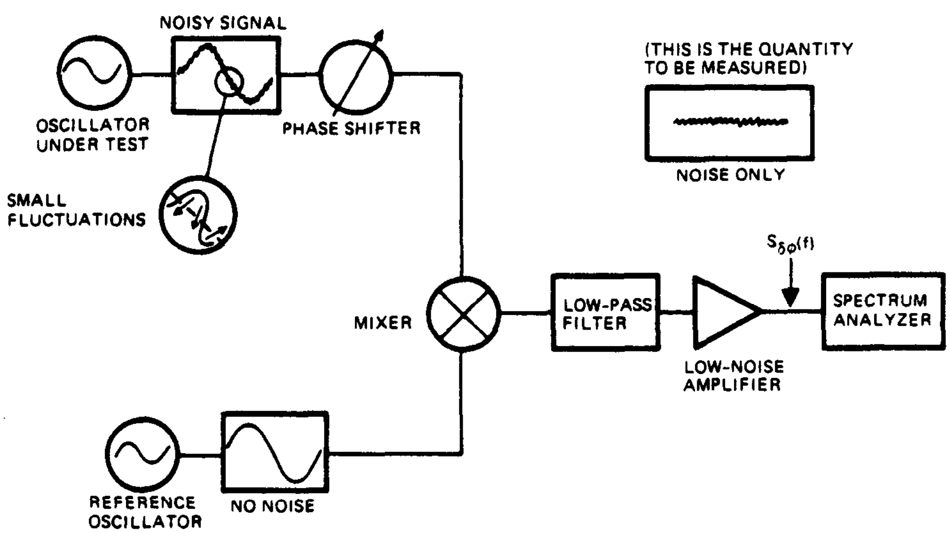

FIG. 8 The two-oscillator technique for measuring phase noise. Small fluctuations from nominal voltage are equivalent to phase variations. The phase shifter adjusts the two signals to quadrature in the mixer, which cancels carriers and converts phase noise to fluctuating dc voltage.

* See Appendix Note # 6

Assume that the reference oscillator is perfect (no phase noise), and that it can be adjusted in frequency. Also, assume that both oscillators are extremely stable, so that phase quadrature can be maintained without the use of an external phase-locked loop or reference. The double-balanced mixer acts as a phase detector so that when two input signals are identical in frequency and are in phase quadrature, the output is a small fluctuating voltage. This represents the phase-modulated (PM) sideband component of the signal because, due to the quadrature of the signals at the mixer input, the mixer converts the amplitude-modulated (AM) sideband components to FM, and at the same time it converts the PM sideband components to AM. These AM components can be detected with an amplitude detector, as shown in Fig. 3.

If the two oscillator signals applied to the double-balanced mixer of Fig. 8 are slightly out of zero beat, a slow sinusoidal voltage with a peak-to-peak voltage V_{ptp} can be measured at the mixer output. If these same signals are returned to zero beat and adjusted for phase quadrature, the output of the mixer is a small fluctuating voltage (δv) centered at zero volts. If the fluctuating voltage is small compared to $\frac{1}{2}V_{\text{ptp}}$, the phase quadrature condition is being closely maintained and the "small angle" condition is being met. Phase fluctuations in radians between the test and reference signals (phases) are

$$\delta\phi = \delta(\phi_t - \phi_r). \tag{52}$$

These phase fluctuations produce voltage fluctuations at the output of the mixer,

$$\delta v = \tfrac{1}{2}V_{\text{ptp}}\,\delta\phi, \tag{53}$$

where phase angles are in radian measure and $\sin\delta\phi = \delta\phi$ for small $\delta\phi$ ($\delta\phi \ll 1$ rad). Solving for $\delta\phi$, squaring both sides, and taking a time average gives

$$\langle(\delta\phi)^2\rangle = 4\langle(\delta v)^2\rangle/(V_{\text{ptp}})^2, \tag{54}$$

where the angle brackets represent the time average.

For the sinusoidal beat signal,

$$(V_{\text{ptp}})^2 = 8(V_{\text{rms}})^2. \tag{55}$$

The mean-square fluctuations of phase $\delta\phi$ and voltage δv interpreted in a spectral density fashion gives the following in radians squared per hertz:

$$S_{\delta\phi}(f) = S_{\delta v}(f)/2(V_{\text{rms}})^2. \tag{56}$$

Here, $S_{\delta v}(f)$, in volts squared per hertz, is the spectral density of the voltage fluctuations at the mixer output. Because the spectrum analyzer measures rms voltage, the noise voltage is in units of volts per square root hertz, which means volts per square root bandwidth. Therefore,

$$S_{\delta v}(f) = [\delta v_{\mathrm{rms}}/\sqrt{B}] = (\delta v_{\mathrm{rms}})^2/B, \tag{57}$$

where B is the noise power bandwidth used in the measurement.

Because it was assumed that the reference oscillator did not contribute any noise, the voltage fluctuations v_{rms} represent the oscillator under test, and the spectral density of the phase fluctuations in terms of the voltage measurements performed with the spectrum analyzer, in radians squared per hertz, is

$$S_{\delta\phi}(f) = \tfrac{1}{2}[(\delta v_{\mathrm{rms}})^2/B(V_{\mathrm{rms}})^2]. \tag{58}$$

Equation (46) is sometimes expressed as

$$S_{\delta\phi}(f) = S_{\delta v}(f)/K^2, \tag{59}$$

where K is the calibration factor in volts per radian. For sinusoidal beat signals, the peak voltage of the signal equals the slope of the zero crossing in volts per radian. Therefore, $(V_{\mathrm{p}})^2 = 2(V_{\mathrm{rms}})^2$, which is the same as the denominator in Eq. (56).

The term $S_{\delta\phi}(f)$ can be expressed in decibels relative to one square radian per hertz by calculating 10 log $S_{\delta\phi}(f)$ of the previous equation:

$$S_{\delta\phi}(f) = 20\log(\delta v_{\mathrm{rms}}) - 20\log(V_{\mathrm{rms}}) - 10\log(B) - 3\,. \tag{60}$$

A correction of 2.5 is required for the tracking spectrum analyzer used in these measurement systems. $\mathscr{L}(f)$ differs by 3 dB and is expressed in decibels (carrier) per hertz as

$$\mathscr{L}(f) = 20\log(\delta v_{\mathrm{rms}}) - 20\log(V_{\mathrm{rms}}) - 10\log(\mathrm{B}) - 6. \tag{61}$$

A. Two Noisy Oscillators

The measurement system of Fig. 6 yields the output noise from both oscillators. If the reference oscillator is superior in performance as assumed in the previous discussions, then one obtains a direct measure of the noise characteristics of the oscillator under test.

If the reference and test oscillators are the same type, a useful approximation is to assume that the measured noise power is twice that associated with one noisy oscillator. This approximation is in error by no more than 3 dB for the noisier oscillator, even if one oscillator is the major source of noise. The equation for the spectral density of measured phase fluctuations in radians squared per hertz is

$$S_{\delta\phi}(f)\bigg|_{\#1} + S_{\delta\phi}(f)\bigg|_{\#2} = \bigg|S_{\delta v}(f)\bigg|_{(\text{two devices})} \div 2(V_{\mathrm{rms}})^2 \doteq \bigg|2S_{\delta\phi}(f)\bigg|_{(\text{one device})} \tag{62}$$

The measured value is therefore divided by two to obtain the value for the single oscillator. A determination of the noise of each oscillator can be made if one has three oscillators that can be measured in all pair combinations. The phase noise of each source 1, 2, and 3 is calculated as follows:

$$\mathscr{L}_1(f) = 10 \log[\tfrac{1}{2}(10^{\mathscr{L}_{12}(f)/10} + 10^{\mathscr{L}_{13}(f)/10} - 10^{\mathscr{L}_{23}(f)/10})], \quad (63)$$

$$\mathscr{L}^2(f) = 10 \log[\tfrac{1}{2}(10^{\mathscr{L}_{12}(f)/10} + 10^{\mathscr{L}_{23}(f)/10} - 10^{\mathscr{L}_{13}(f)/10})], \quad (64)$$

$$\mathscr{L}^3(f) = 10 \log[\tfrac{1}{2}(10^{\mathscr{L}_{13}(f)/10} + 10^{\mathscr{L}_{23}(f)/10} - 10^{\mathscr{L}_{12}(f)/10})]. \quad (65)$$

B. Automated Phase-Noise Measurements Using the Two-Oscillator Technique

The automated phase-noise measurement system is shown in Fig. 9. It is controlled by a programmable calculator. Each step of the calibration and measurement sequence is included in the program. The software program controls frequency slection, bandwidth settings, settling time, amplitude ranging, measurements, calculations, graphics, and data plotting. Normally, the system is used to obtain a direct plot of $\mathscr{L}(f)$. The integrated phase noise can be calculated for any selected range of Fourier frequencies.

A quasi-continuous plot of phase noise performance $\mathscr{L}(f)$ is obtained by performing measurements at Fourier frequencies separated by the IF bandwidth of the spectrum analyzer used during the measurement. Plots of other defined parameters can be obtained and plotted as desired.

The IF bandwidth settings for the Fourier (offset) frequency-range selections are shown in the following tabulation:

IF bandwidth (Hz)	Fourier frequency (kHz)	IF bandwidth (kHz)	Fourier frequency (kHz)
3	0.001–0.4	1	40–100
10	0.4–1	3	100–400
30	1–4	10	400–1300
100	4–10		
200	10–40		

The particular range of Fourier frequencies is limited by the particular spectrum analyzer used in the system. A fast Fourier analyzer (FFT) is also incorporated in the system to measure phase noise from submillihertz to 25 kHz.

High-quality sources can be measured without multiplication to enhance the phase noise prior to downconverting and measuring at baseband frequencies. The measurements are not completely automated because the calibration sequence requires several manual operations.

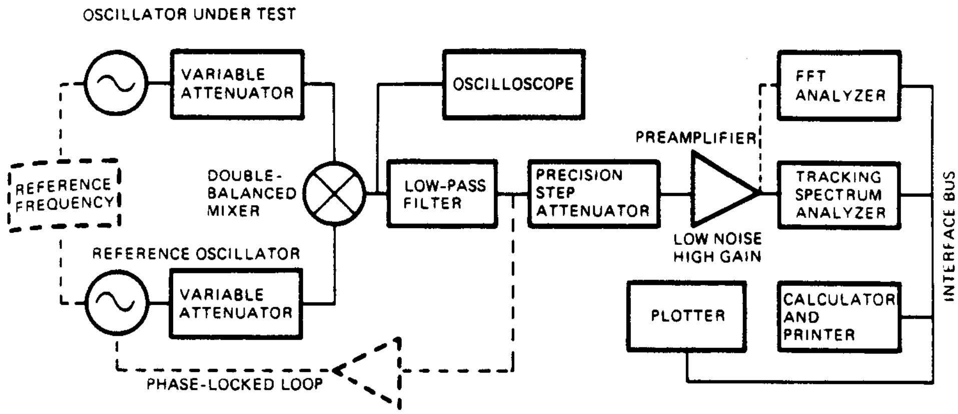

FIG. 9 An automated phase-noise measurement system.

C. Calibration and Measurements Using the Two-Oscillator System

$\mathcal{L}(f)$ is a normalized frequency domain measure of phase-fluctuation side-band power. The noise power is measured relative to the carrier power level. Correction must be applied because of the type of measurement and the characteristics of the measurement equipment. The general procedure for the calibration and measurement sequence includes the following: measuring the noise power bandwidth for each IF bandwidth setting on the Tracking Spectrum Analyzer (Section III.C.1); establishing a carrier reference power level referenced to the output of the mixer (Section III.C.2); obtaining phase quadrature of the two signals applied to the mixer (Section III.C.3); measuring the noise power at the selected Fourier frequencies (Section III.C.4); performing the calculations and plotting the data (Section III.C.5); and measuring the system noise floor characteristics, usually referred to as the system sensitivity.

1. *Noise-Power Bandwidth*

Approximations of analyzer-noise bandwidths are not adequate for phase noise measurements and calculations. The IF noise-power bandwidth of the tracking spectrum analyzer must be *known* and used in the calculations of phase noise parameters. Figure 10 shows the results of measurements performed using automated techniques. For example, with a 1-MHz signal input to the tracking spectrum analyzer, the desired incremental frequency changes covering the IF bandwidth are set by calculator control.

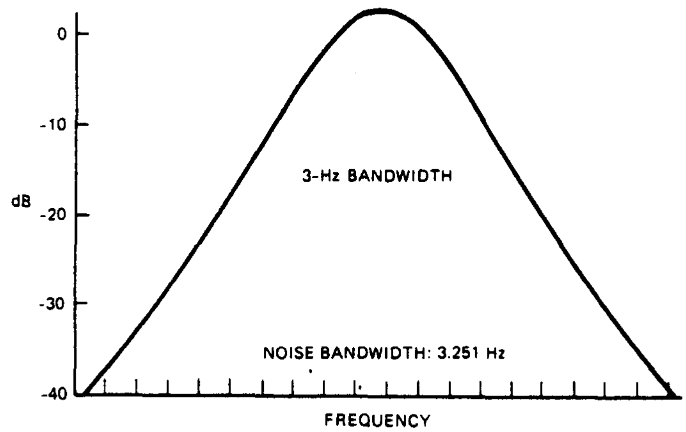

FIG. 10 Plot of automated noise-power bandwidth.

The spectrum analyzer power output is recorded for each frequency setting over the range, as illustrated in Fig. 10. The 40-dB level and the 100 increments in frequency are not the minimum permissible values. The recorded can be plotted for each IF bandwidth, as illustrated, and the noise-power bandwidth is calculated in hertz as

$$\text{noise power bandwidth} = \frac{(P_1 + P_2 + P_3 + \cdots + P^{100})\,\Delta f}{\text{peak power reading}}, \qquad (66)$$

where Δf is the frequency increment in hertz and the peak power is the maximum measured point obtained during the measurements. All power values are in watts.

2. *Setting the Carrier Power Reference Level*

Recall from Section III.6 that for sinusoidal signals the peak voltage of the signal equals the slope of the zero crossing, in volts per radian. A frequency offset is established, and the peak power of the difference frequency is measured as the carrier-power reference level; this establishes the calibration factor of the mixer in volts per radian.

Because the precision IF attenuator is used in the calibration process, one must be aware that the impedance looking back into the mixer should be 50 Ω. Also, the mixer output signal should be sinusoidal. Fischer (1978) discussed the mixer as the "critical element" in the measurement system. It is advisable to drive the mixer so that the sinusoidal signal is obtained at the mixer output. In most of the TRW systems, the mixer drive levels are 10 dBm for the reference signal and about zero dBm for the unit under test.

System sensitivity can be increased by driving the mixer with high-level signals that lower the mixer output impedance to a few ohms. This presents a problem in establishing the calibration factor of the mixer, because it might be necessary to calibrate the mixer for different Fourier frequency ranges.

The equation sensitivity = slope = beat-note amplitude does not hold if the output of the mixer is not a sine wave. The Hewlett-Packard 3047 automated phase noise measurement system allows accurate calibration of the phase-detector sensitivity even with high-level inputs by using the derivative of the Fourier representation of the signal (the fundamental and its harmonics). The slope at $\phi \cong 0$ radians is given by

$$\begin{aligned} A \sin \phi - B \sin 3\phi + C \sin 5\phi &= A \cos \phi - 3B \cos 3\phi + 5C \cos 5\phi \\ &= A - 3B + 5C + \cdots. \end{aligned} \tag{67}$$

Referring to Fig. 9, the carrier-power reference level is obtained as follows.

(1) The precision IF step attenuator is set to a high value to prevent overloading the spectrum analyzer (assume 50 dB as our example).

(2) The reference and test signals at the mixer inputs are set to approximately 10 dBm and 0 dBm, as previously discussed.

(3) If the frequency of one of the oscillators can be adjusted, adjust its frequency for an IF output frequency in the range of 10 to 20 kHz. If neither oscillator is adjustable, replace the oscillator under test with one that can be adjusted as required and that can be set to the identical power level of the oscillator under test.

(4) The resulting IF power level is measured by the spectrum analyzer, and the measured value is corrected for the attentuator setting, which was assumed to be 50 dB. The correction is necessary because this attenuator will be set to its zero decibel indication during the measurements of noise power. Assuming a spectrum analyzer reading of -40 dBm, the carrier-power reference level is calculated as

$$\text{carrier power reference level} = 50\text{ dB} - 40\text{ dBm} = 10\text{ dBm}. \tag{68}$$

3. *Phase Quadrature of the Mixer Input Signals*

After the carrier-power reference has been established, the oscillator under test and the reference oscillator are tuned to the same frequency, and the original reference levels that were used during calibration are reestablished. The quadrature adjustment depends on the type of system used. Three possibilities, illustrated in Fig. 9, are described here.

(1) If the oscillators are very stable, have high-resolution tuning, and are not phase-locked, the frequency of one oscillator is adjusted for *zero dc*

voltage output of the mixer as indicated by the sensitive oscilloscope. Note: Experience has shown that the quadrature setting is not critical if the sources have low AM noise characteristics. As an example, experiments performed using two HP 3335 synthesizers showed that degradation of the phase-noise measurement became noticeable with a phase-quadrature offset of 16 degrees.

(2) If the common reference frequency is used, as illustrated in Fig. 9, then it is necessary to include a phase shifter in the line between one of the oscillators and the mixer (preferably between the attenuator and mixer). The phase shifter is adjusted to obtain and maintain zero volts dc at the mixer output. A correction for a nonzero dc value can be applied as exemplified by the HP 3047 automated phase-noise measurement system.

(3) If one oscillator is phase-locked using a phase-locked loop, as shown dotted in on Fig. 9, the frequency of the unit under test is adjusted for zero dc output of the mixer as indicated on the oscilloscope.

A phase-locked loop is a feedback system whose function is to force a voltage-controlled oscillator (VCO) to be coherent with a certain frequency, i.e., it is highly correlated in both frequency and phase. The phase detector is a mixer circuit that mixes the input signal with the VCO signal. The mixer output is $\nu_i \pm \nu_0$. when the loop is locked, the VCO duplicates the input frequency so that the difference frequency is zero, and the output is a dc voltage proportional to the phase difference. The low-pass filter removes the sum frequency component but passes the dc component to control the VCO. The time constant of the loop can be adjusted as needed by varying amplifier gain and RC filtering within the loop.

A *loose phase-locked loop* is characterized by the following.

(1) The correction voltage varies as phase (in the short term) and phase variations are therefore observed directly.

(2) The bandwidth of the servo response is small compared with the Fourier frequency to be measured.

(3) The response time is very slow.

A *tight phase-locked loop* is characterized by the following.

(1) The correction voltage of the servo loop varies as frequency.

(2) The bandwidth of the servo response is relatively large.

(3) The response time is much smaller than the smallest time interval τ at which measurements are performed.

Figure 11 shows the phase-noise characteristics of the H.P. 8640B synthesizer measured at 512 MHz. The phase-locked-loop attenuation characteristics extend to 10 kHz. The internal-oscillator-source characteristics are plotted at Fourier frequencies beyond the loop-bandwidth cutoff at 10 kHz.

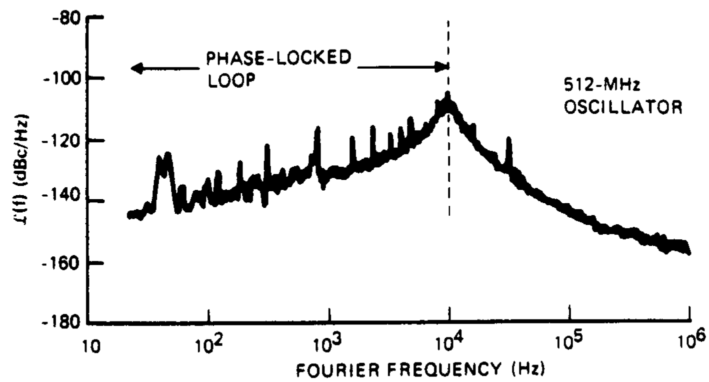

FIG. 11 Phase-locked-loop characteristics of the H.P. 8640B signal generator, showing the normalized phase-noise sideband power spectral density.

4. *Measurements, Calculations, and Data Plots*

The measurement sequence is automated except for the case where manual adjustments are required to maintain phase quadrature of the signals. After phase quadrature of the signals into the mixer is established, the IF attenuator is returned to the zero-decibel reference setting. This attenuator is set to a high value [assumed to be 50 dB in Eq. (65)] to prevent saturation of the spectrum analyzer during the calibration process.

The automated measurements are executed, and the direct measurement and data plot of $\mathscr{L}(f)$ is obtained in decibels (carrier) per hertz using the equation

$$\mathscr{L}(f) = -\,[\text{carrier power level} - (\text{noise power level} - 6 + 2.5 - 10 \log B - 3)]. \tag{69}$$

The noise power (dBm) is measured relative to the carrier-power level (dBm), and the remaining terms of the equation represent corrections that must be applied because of the type of measurement and the characteristics of the measurement equipment, as follows.

(1) The measurement of noise sidebands with the signals in phase quadrature requires the -6-dB correction that is noted in Eq. (69).

(2) The nonlinearity of the spectrum analyzer's logarithmic IF amplifier results in compression of the noise peaks which, when average-detected, require the 2.5-dB correction.

(3) The bandwidth correction is required because the spectrum analyzer measurements of random or white noise are a function of the particular bandwidth used in the measurement.

(4) The -3-dB correction is required because this is a direct measure of $\mathscr{L}(f)$ of *two oscillators*, assuming that the oscillators are of a similar type and that the noise contribution is the same for each oscillator. If one oscillator is sufficiently superior to the other, this correction is not required.

Other defined spectral densities can be calculated and plotted as desired. The plotted or stored value of the spectral density of phase fluctuations in decibels relative to one square radian (dBc rad^2/Hz) is calculated as

$$S_{\delta\phi}(f) = \mathscr{L}(f) + 3. \tag{70}$$

The spectral density of phase fluctuations, in radians squared per hertz, is calculated as

$$S_{\delta\phi}(f) = 10\exp(S_{\delta\phi}(f)/10), \tag{71}$$

The spectral density of frequency fluctuations, in hertz squared per hertz, is

$$S_{\delta\nu}(f) = f^2 S_{\delta\phi}(f). \tag{72}$$

where $S_{\delta\phi}(F)$ is in decibels with respect to 1 radian.

5. *System Noise Floor Verification*

A plot of the system noise floor (sensitivity) is obtained by repeating the automated measurement procedures with the system modified as shown in Fig. 12. Accurate measurements can be obtained using the configuration shown in Fig. 12a. The reference source supplies 10 dBm to one side of the mixer and 0 dBm to the other mixer input through equal path lengths; phase quadrature is maintained with the phase shifter.

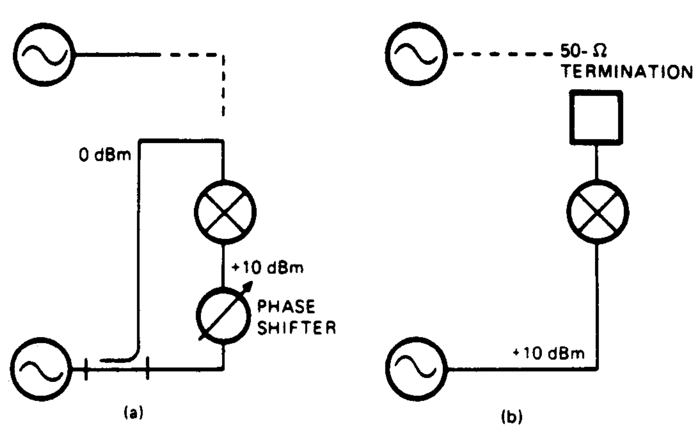

FIG. 12 System configurations for measuring the system noise floor (sensitivity): (a) configuration used for accurate measurements; (b) alternate configuration sometimes used.

The configuration shown in Fig. 12b is sometimes used and does not greatly degrade the noise floor because the reference signal of 10 dBm is larger than the signal frequency. See Sections IV.B and IV.C.4 for additional discussions related to system sensitivity and recommended system evaluation.

Proper selection of drive and output termination of the double-balanced mixer can result in improvement by 15 to 25 dB in the performance of phase-noise measurements, as discussed by Walls *et al.* (1976). The beat frequency between the two oscillators can be a sine wave, as previously mentioned, with proper low drive levels. This requires a proper terminating impedance for the mixer. With high drive levels, the mixer output waveform will be clipped. The slope of the clipped waveform at the zero crossings, illustrated by Walls *et al.* (1976), is twice the slope of the sine wave and therefore improves the noise floor sensitivity by 6 dB, i.e., the output signal, proportional to the phase fluctuations, increases with drive level. This condition of clipping requires characterization over the Fourier frequency range, as previously mentioned for the Hewlett-Packard 3047 phase noise measurement system. An amplifier can be used to increase the mixer drive levels for devices that have insufficient output power to drive the double-balanced mixers.

Lower noise floors can be achieved using high-level mixers when available drive levels are sufficient. A step-up transformer can be used to increase the mixer drive voltage because the signal and noise power increase in the same ratio, and the spectral density of phase of the device under test is unchanged, but the noise floor of the measurement system is reduced.

Walls *et al.* (1976) used a correlation technique that consisted primarily of two phase-noise measurement systems. At TRW the technique is used as shown in Fig. 13. The cross spectrum is obtained with the fast Fourier transform (FFT) analyzer that performs the product of the Fourier transform of one signal and the complex conjugate of the Fourier transform of

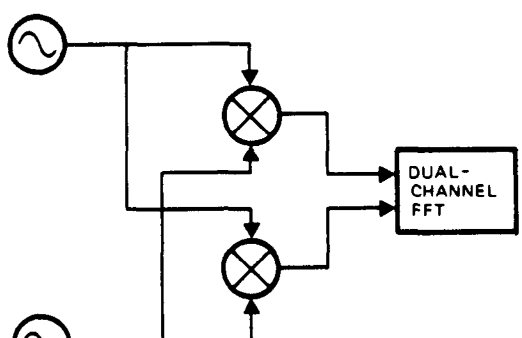

FIG. 13 Cross-spectrum measurement using the two-oscillator technique.

the second signal. This cross spectrum, which is a phase-sensitive characteristic, gives a phase and amplitude sensitivity measure directly. A signal-to-noise enhancement greater than 20 dB can be achieved.

If the double-balanced phase noise measurement system does not provide a noise floor sufficient for measuring a high-quality source, frequency multiplier chains can be used if their inherent noise is 10–20 dB below the measurement system noise. In frequency multiplication the noise increases according to

$$10 \log(\text{final frequency}/\text{original frequency}). \qquad (73)\ *$$

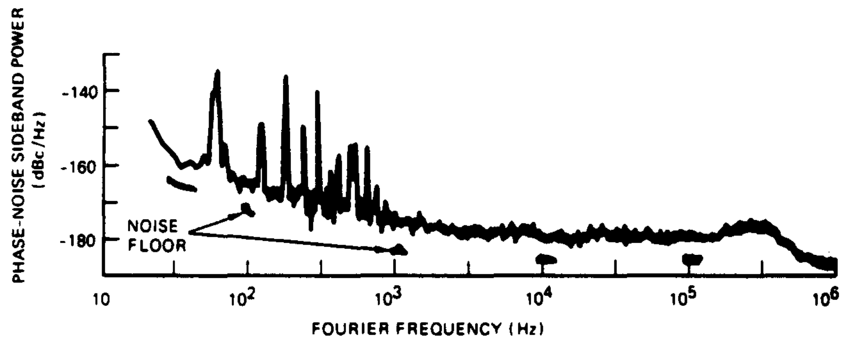

(a)

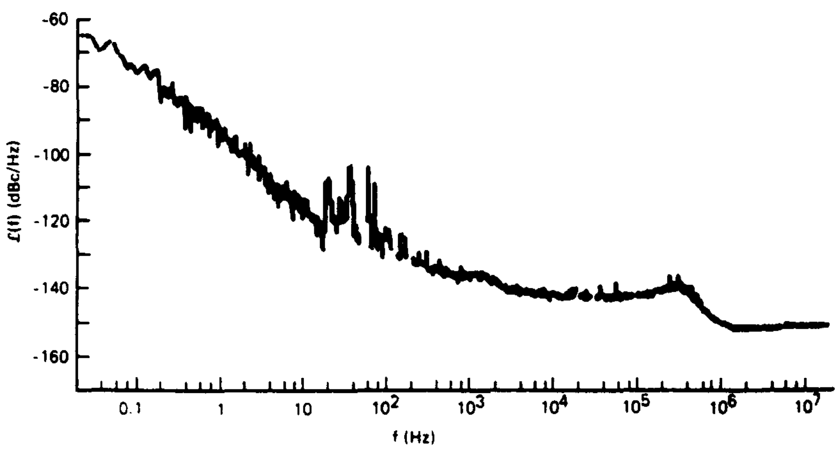

(b)

FIG. 14 Data plots of the automated phase-noise measurement system: (a) a high quality 5-MHz quartz oscillator; (b) combined noise of two H.P. 8662A synthesizers (subtract 3 dB for a single unit).

* See Appendix Note # 32

The following equation is used to correct for noise-floor contribution P_{nf}, in dBc/Hz, if desired or necessary:

$$\mathscr{L}(f)(\text{corrected}) = -\mathscr{L}(f) + 10 \log\left[\frac{P_{\mathscr{L}(f)} - P_{nf}}{P_{\mathscr{L}(f)}}\right] \tag{74}$$

The correction for noise-floor contribution can also be obtained by using the measurement of $S_{\delta v}(f)$ of Eq. (57). Measurement of $S_{\delta v}(f)$ of the oscillator plus floor is obtained, then $S_{\delta v}(f)$ is obtained for the noise floor only. Then,

$$S_{\delta v}(f)\Big|_{\text{cor}} = S_{\delta v}(f)\Big|_{(\text{osc}+\text{nf})} - S_{\delta v}(f)\Big|_{\text{nf}} \tag{75}$$

Figure 14a shows a phase noise plot of a very high-quality (5-MHz) quartz oscillator, measured by the two-oscillator technique. The sharp peaks below 1000 Hz represent the 60-Hz line frequency of the power supply and its harmonics and are not part of the oscillator phase noise. Figure 14b shows measurements to 0.02 Hz of the carrier at a frequency of 20 MHz.

IV. Single-Oscillator Phase-Noise Measurement Systems and Techniques *

The phase-noise measurements of a single-oscillator are based on the measurement of *frequency fluctuations* using discriminator techniques. The practical discriminator acts as a filter with finite bandwidth that suppresses the carrier and the sidebands on both sides of the carrier. The ideal carrier-suppression filter would provide infinite attentuation of the carrier and zero attenutation of all other frequencies. The effective Q of the practical discriminator determines how much the signals are attenuated.

Frequency discrimination at very high frequencies (VHF) has been obtained using slope detectors and ratio detectors, by use of lumped circuit elements of inductance and capacitance. At ultrahigh frequencies (UHF) between the VHF and microwave regions, measurements can be performed by beating, or heterodyning, the UHF signal with a local oscillator to obtain a VHF signal that is analyzed with a discriminator in the VHF frequency range. Those techniques provide a means for rejecting residual amplitude-modulated (AM) noise on the signal under test. The VHF discriminators usually employ a limiter or ratio detector.

Ashley *et al.* (1968) and Ondria (1968) have discussed the microwave cavity discriminator that rejects AM noise, suppresses the carrier so that the input level can be increased, and provides a high discriminated output to improve the signal-to-noise floor ratio. The delay line used as an FM discriminator has been discussed by Tykulsky (1966), Halford (1975), and

* See Appendix Note # 6

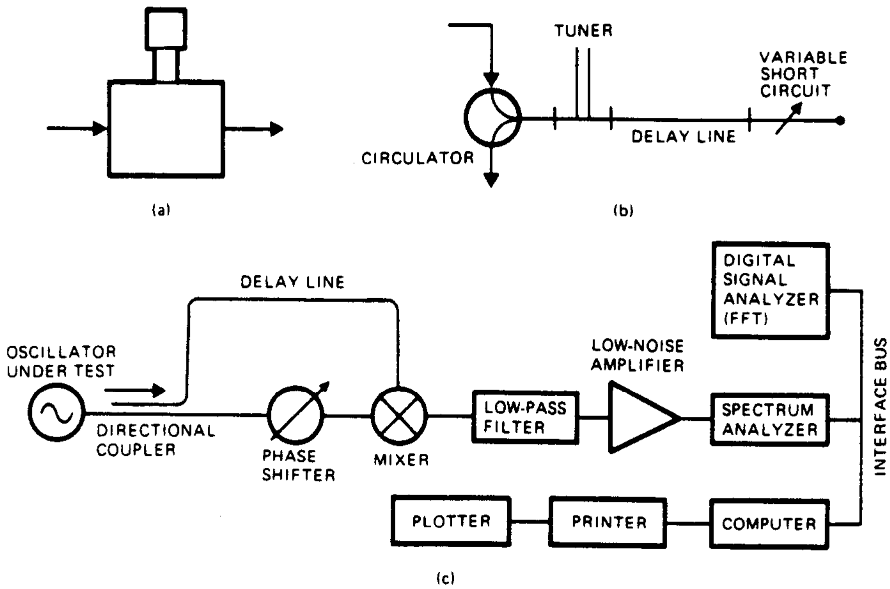

FIG. 15 Single-oscillator phase-noise measurement techniques: (a) cavity discriminator; (b) reflective-type delay-line discriminator; (c) one-way delay line.

Ashley *et al.* (1968). Ashley *et al.* (1968) proposed the reflective-type delay-line discriminator shown in Fig. 15b. The cavity can also be used to replace delay line. The one-way delay line shown in Fig. 15c is implemented in the TRW measurement systems. The theory and applications set forth in this section are based on a system of this particular type.

A. THE DELAY LINE AS AN FM DISCRIMINATOR

1. *The Single-Oscillator Measurement System*

The single-oscillator signal is split into two channels in the system shown in Fig. 15. One channel is called the nondelay or reference channel. It is also referred to as the local-oscillator (LO) channel because the signal in this channel drives the mixer at the prescribed impedance level (the usual LO drive). The signal in the second channel arrives at the mixer through a delay line. The two signals are adjusted for phase quadrature with the phase shifter, and the output of the mixer is a fluctuating voltage, analogous to the frequency fluctuations of the source, centered on approximately zero dc volts.

The delay line yields a phase shift by the time the signal arrives at the balanced mixer. The phase shift depends on the instantaneous frequency of the signal. The presence of frequency modulation (FM) on the signal gives rise to differential phase modulation (PM) at the output of the differential delay and its associated (nondelay) reference line. This relationship is linear if the delay τ_d is nondispersive. This is the property that allows the delay line to be used as an FM discriminator. In general, the conversion factors are a function of the delay (τ_d) and the Fourier frequency f but not of the carrier frequency.

The differential phase shift of the nominal frequency ν_0 caused by the delay line is

$$\Delta\phi = 2\pi\nu_0\tau_d, \tag{76}$$

where τ_d is the time delay.

The phase fluctuations at the mixer are related to the frequency fluctuations (at the rate f) by

$$\delta\phi = 2\pi\tau_d\,\delta\nu(f). \tag{77}$$

The spectral density relationships are

$$S_{\delta\phi}(f)\Big|_{\text{mixer}} = (2\pi\tau_d)^2\, S_{\delta\nu}(f)\Big|_{\text{osc}} \tag{78}$$

and

$$S_{\delta\nu}(f) = f^2\, S_{\delta\phi}(f). \tag{79}$$

Then,

$$S_{\delta\phi}(f)\Big|_{\text{dlm}} = (2\pi f\tau_d)^2\, S_{\delta\phi}(f)\Big|_{\text{osc}} \tag{80}$$

where the subscript dlm indicates delay-line method. From Eq. (56), the spectral density of phase for the two-oscillator technique, in radians squared per hertz, is

$$S_{\delta\phi}(f) = 4\,\frac{S_{\delta v}(f)}{(V_{\text{ptp}})^2} = \frac{S_{\delta v}(f)}{2(V_{\text{rms}})^2} = \left[\frac{(\delta v_{\text{rms}})^2}{2(V_{\text{rms}})B}\right] \tag{81}$$

because

$$(V_{\text{ptp}})^2 = 8(v_{\text{rms}})^2 = 4(V_p)^2 = 4[2(v_{\text{rms}})^2]$$

and

$$\mathscr{L}(f) = 2(S_{\delta v}(f)/(V_{\text{ptp}})^2) = (\delta v_{\text{rms}})^2/4(V_{\text{rms}})^2 B \tag{82}$$

per hertz.

The sensitivity (noise floor) of the two-oscillator measurement system includes the thermal and shot noise of the mixer and the noise of the base-band preamplifier (referred to its input). This noise floor is measured with the oscillator under test inoperative. The measurement system sensitivity of the two-oscillator system, on a per hertz density basis (dBc/Hz) is

$$\mathscr{L}(f)_{\mathrm{nf}} = 10 \log[2(\delta v_n)^2/(V_{\mathrm{ptp}})^2], \tag{83}$$

where δv_n is the rms noise voltage measured in a one-hertz bandwidth.

The two-oscillator system therefore yields the output noise from both oscillators. If the reference oscillator is superior in performance, as assumed in the previous discussions, then one obtains a direct measure of the noise characteristics of the oscillator under test. If the reference and test oscillators are the same type, a useful approximation is to assume that the measured noise power is twice that associated with one noisy oscillator. This approximation is in error by no more than 3 dB for the noisier oscillator. Substituting in Eq. (80) and using the relationships in Eq. (56), we have, per hertz,

$$\mathscr{L}(f)\Big|_{\mathrm{dlm}} = 2[(\delta v_{\mathrm{rms}})^2/(V_{\mathrm{ptp}})^2](2\pi f\tau_{\mathrm{d}})^2 \tag{84}$$

Examination of this equation reveals the following.

(1) The term in the brackets represents the two-oscillator response. *Note that this term represents the noise floor of the two-oscillator method.* Therefore, adoption of the delay-line method results in a higher noise by the factor $(2\pi f\tau_{\mathrm{d}})^2$ when compared with the two-oscillator measurement method. The sensitivity (noise floor) for delay lines with different values of time delay are illustrated in Fig. 17.

(2) Equation (84) also indicates that the measured value of $\mathscr{L}(f)$ is periodic in $\omega = 2\pi f$. This is shown in Fig. 21. The first null in the responses is at the Fourier frequency $f = 1/\tau_{\mathrm{d}}$. The periodicity indicates that the calibration range of the discriminator is limited and that valid measurements occur only in the indicated range, as verified by the discriminator slope shown in Fig. 16. (See Fig. 23.)

(3) The maximum value of $(2\pi f\tau_{\mathrm{d}})^2$ can be greater than unity (it is 4 at $f = 1/2\tau_{\mathrm{d}}$). This 6-dB advantage is utilized in the noise-floor measurement. However, it is beyond the valid calibration range of the delay-line system. The 6-dB advantage is offset by the line attenuation at microwave frequencies, as discussed by Halford (1975).

The delay-line discriminator system has been analyzed in terms of a power-limited system (a particular idealized system in which the choice of power oscillator voltage, the attenuator of the delay line, and the conversion loss of the mixer are limited by the capability of the mixer) by Tykulsky (1966), Halford (1975), and Ashley *et al.* (1977). For this particular case, Eq. (83) indicates that an increase in the length of the delay line (to increase τ_d for decorrelation of Fourier frequencies closer to the carrier) results in an increase in attenuation of the line, which causes a corresponding decrease in V_{ptp}. The optimum length occurs where τ_d is such that the decrease in V_{ptp} is approximately compensated by the increase in $(2\pi f \tau_d)$, i.e., where

$$\frac{d}{d\tau_d}\frac{2\pi f \tau_d}{V_{ptp}} = 0. \tag{85}$$

This condition occurs where the attenuation of the delay line is 1 Np (8.686 dB). However, when the system is not power limited, the attenuation of the delay line is not limited, because the input power to the delay line can be adjusted to maintain V_{ptp} at the desired value. The optimum delay-line length is determined at a particular selectable frequency. However, since the attenuation varies slowly (approximately proportional to the square root of frequency), this characteristic allows near-optimum operation over a considerable frequency range without appreciable degradation in the measurements.

A practical view of the time delay (τ_d) and Fourier-frequency functional relationship can be obtained by reviewing the basic concepts of the dual-channel time-delay measurement system discussed by Lance (1964). If the differential delay between the two channels is zero, there is no phase difference at the detector output when a swept-frequency cw signal is applied to the system. Figure 16 shows the detected output interference display when a swept-frequency cw signal (zero to 4 MHz) is applied to a system that has

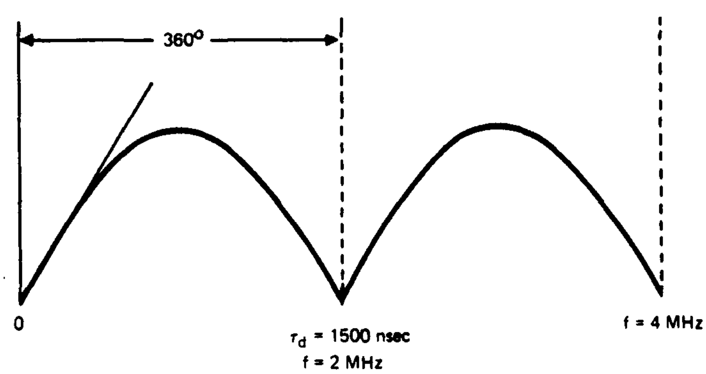

FIG. 16 Swept-frequency interference display at the output of a dual-channel system with a differential delay of 500 nsec.

a differential delay of 500 nsec between the two channels. The signal amplitudes are assumed to be almost equal, thus producing the familiar voltage-standing-wave pattern or interference display. Because this is a two-channel system, there is a null every 360°, as shown.

2. *System Sensitivity (Noise Floor) When Using the Differential Delay-Line Technique*

Halford (1975) has shown that the sensitivity (noise floor) of the single-oscillator differential delay-line technique is reduced relative to the two-oscillator techniques. The sensitivity is modified by the factor

$$S_d = 2(1 - \cos 2\pi f \tau_d). \tag{86}$$

For $\omega\tau_d = 2\pi d\tau_d \ll 1$ a good approximation is

$$S_d^2 = 2(1 - \cos 2\pi f \tau_d) = (\omega\tau_d)^2[1 - \tfrac{1}{12}(\omega\tau_d)^2] = (2\pi f \tau_d)^2 = \theta^2, \tag{87}$$

where θ is the phase delay of the differential delay line evaluated at the frequency f. Figure 17 shows the relative sensitivity (noise floor) of the two-oscillator technique and the single-oscillator technique with different delay-line lengths. The f^{-2} slope is noted at Fourier frequencies beyond

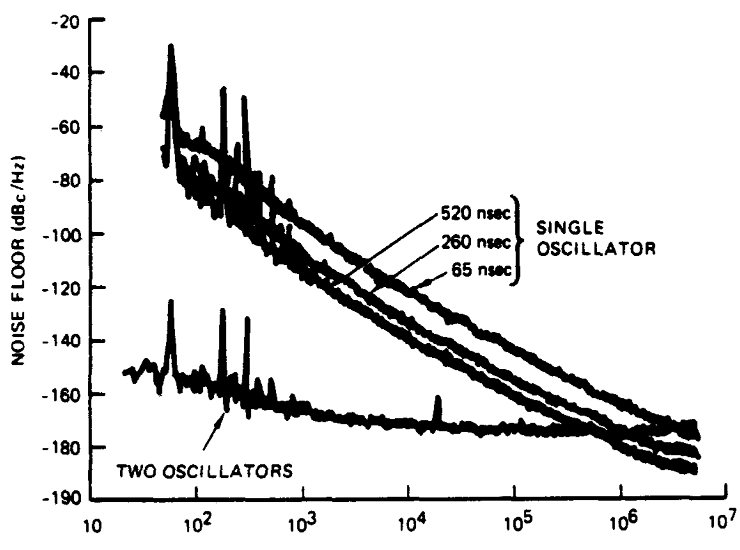

FIG. 17 Relative sensitivity (noise floor) of single-oscillator and two-oscillator phase-noise measurement systems.

about 1 kHz. For Fourier frequencies closer to the carrier, the slope is f^{-3}, i.e., the sum of the f^{-2} slope of Eq. (87) and the f^{-1} flicker noise.

Phase-locked sources have phase-noise characteristics that cannot be measured at close-in Fourier frequencies using this basic system. The relative sensitivity of the system can be improved by using a dual (two-channel) delay-line system and performing cross-spectrum analysis, which will be presented in this chapter.

Labaar (1982) developed the delay-line rf bridge configuration shown in Fig. 18. At microwave frequencies where a high-gain amplifier is available, suppression of the carrier by the rf bridge allows amplification of the noise going into the mixer. A relative sensitivity improvement of 35 dB has been obtained without difficulty. The limitations of the technique depend on the available rf power and the carrier suppression by the bridge. Naturally, if the rf input to the bridge is high one must use the technique with adequate precautions to prevent mixer damage that can occur by an accidental bridge unbalance. Labaar (1982) indicated the added advantage of using the rf bridge carrier-suppression technique when attempting to measure phase noise close to the carrier when AM noise is present. Figure 19 shows the

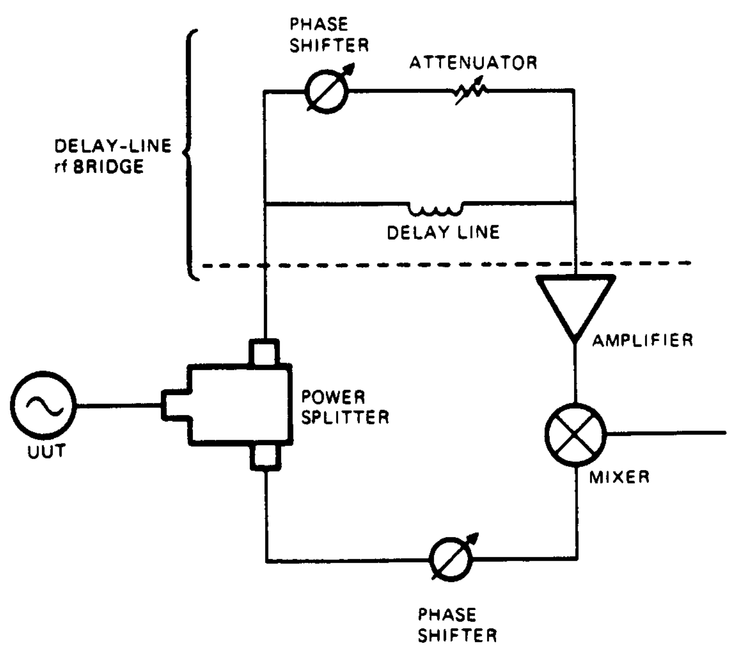

FIG. 18 Carrier suppression using an rf bridge to increase relative sensitivity. (Courtesy Instrument Society of America.)

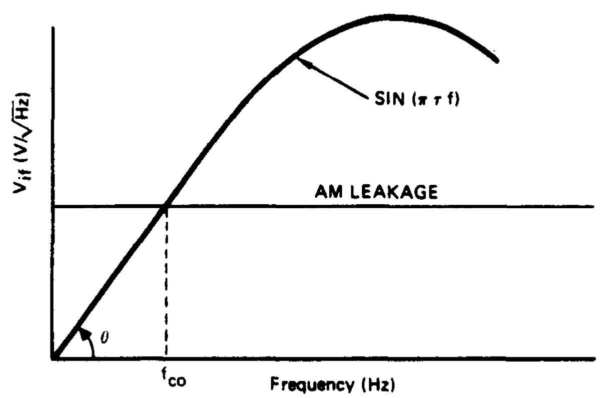

FIG. 19 Phase detector output (AM-PM crossover); τ, delay time.

mixer output for phase (PM) and amplitude (AM) noise in the single-oscillator delay-line FM discriminator system. It is noted that the phase noise and AM noise intersect and that the AM will therefore limit the measurement accuracy near the carrier. Even though AM noise is much lower than phase noise in most sources, and even though the AM is normally suppressed about 20 dB, there is still AM at the mixer output. This output is AM leakage and is caused by the finite isolation between the mixer ports. The two-oscillator technique does not experience this problem to this extent because the phase noise and AM noise maintain their relative relationships at the mixer output independent of the offset frequency from the carrier.

B. Calibration and Measurements Using the Delay Line as an FM Discriminator

The block diagram of a practical single-oscillator phase noise measurement system is shown in Fig. 20. The signals in the delay-line channel of the system experience the one-way delay of the line. With adequate source power, the system is not limited to the optimum 1 Np (8.686 dB) previously discussed for a power-limited system. Measurements are performed using the following operational procedures.

(1) Measure the tracking spectrum analyzer IF bandwidths as set forth in Section III.C.1.

(2) Establish the system power levels (Section IV.B.1).

(3) Establish the discriminator calibration factor (Section IV.B.2).

(4) Measure and plot the oscillator characteristics in the automatic system used (Section IV.B.3).

(5) Measure the system noise floor (sensitivity) (Section IV.B.4).

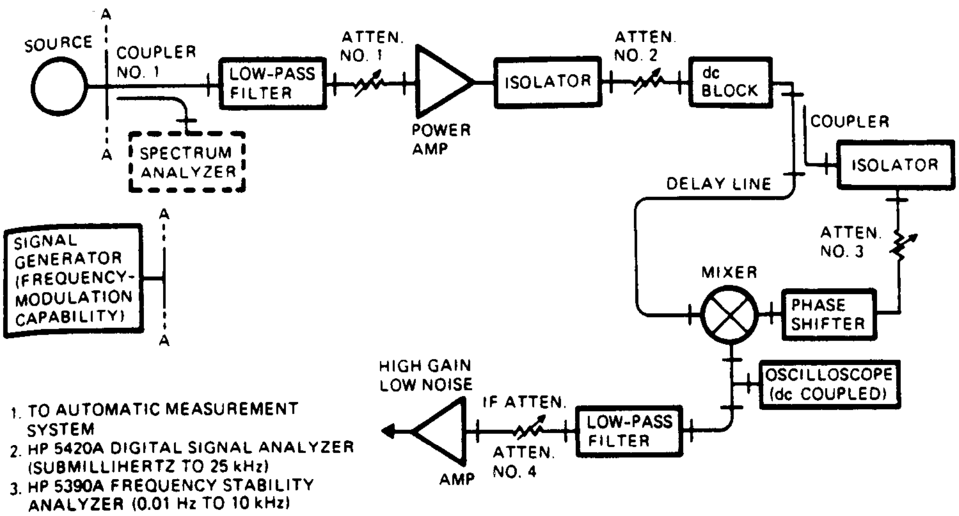

FIG. 20 Single-oscillator phase noise measurement system using the delay line as an FM discriminator. (From Lance *et al.*, 1977a.)

1. *System Power Levels*

The system power levels are set using attenuators, as shown in Fig. 20. Because the characteristic impedance of attenuator No. 4 is 50 Ω, mismatch errors will occur if the mixer output impedance is not 50 Ω. As previously discussed, the mixer drive levels are set so that the mixer output signal, as observed during calibration, is sinusoidal. This has been accomplished in TRW systems with a reference (LO) signal level of 10 dBm and a mixer input level of about 0 dBm from the delay line.

A power amplifier can be used to increase the source signal to the measurement system. This amplifier must not contribute appreciable additional noise to the signal.

2. *Discriminator Calibration*

The discriminator characteristics are measured as a function of frequency and voltage. The hertz-per-volt sensitivity of the discriminator is defined as the *calibration factor* (CF). The calibration process involves measuring the effects of intentional modulation of the source (carrier) frequency. A known modulation index must be obtained to calculate the calibration factors of the discriminator. The modulation index is obtained by using amplitude modulation to establish the carrier-to-sideband ratio when there is considerable instability of the source or when the source cannot be frequency modulated.

It is convenient to consider the system equations and calibration techniques in terms of frequency modulation of stable sources. If the source to be measured cannot be frequency modulated, it must be replaced, during the calibration process, with a modulatable source. The calibration process will be described using a modulatable source and a 20-kHz modulation frequency. However, other modulation frequencies can be used. The calibration factor of this type discriminator has been found to be constant over the usable Fourier frequency range, within the resolution of the measuring technique. The calibration factor of the discriminator is established after the system power levels have been set with the unit under test as the source.

The discriminator calibration procedures are as follows.

(1) Set attenuator No. 4 (Fig. 20) to 50 dB.

(2) Replace the oscillator under test with a signal generator or oscillator that can be frequency modulated. *The power output and operating frequency of the generator must be set to the same precise frequency and amplitude values that the oscillator under test will present to the system during the measurement process.*

(3) Select a modulation frequency of 20 kHz and increase the modulation until the carrier is reduced to the first Bessel null, as indicated on the spectrum analyzer connected to coupler No. 1. This establishes a modulation index ($m = 2.405$).

(4) Adjust the phase shifter for zero volts dc at the output of the mixer, as indicated on the oscilloscope connected as shown in Fig. 20. *This establishes the quadrature condition for the two inputs to the mixer.* This quadrature condition is continuously monitored and is adjusted if necessary.

(5) Tune the tracking spectrum analyzer to the modulation frequency of 20 kHz. The power reading at this frequency is recorded in the program and is corrected for the 50-dB setting of attenuator No. 4, which will be set to zero decibel indication during the automated measurements.

$$P(\mathrm{dBm}) = (-\mathrm{dBm\ power\ reading}) + 50\ \mathrm{dB} \tag{88}$$

This power level is converted to the equivalent rms voltage that the spectrum analyzer would have read if the total signal had been applied:

$$V_{\mathrm{rms}} = \sqrt{10^{P/10}/1000 + R}. \tag{89}$$

(6) The discriminator calibration factor can now be calculated because this power in dBm can be converted to the corresponding rms voltage using the following equation:

$$V_{\mathrm{rms}} = \sqrt{(10^{P/10}/1000) \times R}, \tag{90}$$

where $R = 50\ \Omega$ in this system.

(7) The discriminator calibration factor is calculated in hertz per volt as

$$CF = mf_m/\sqrt{2}\,V_{rms} = 2.405 f_m/\sqrt{2}\,V_{rms}. \tag{91}$$

The modulation index m for the first Bessel null as used in this technique is 2.405. The modulation frequency is f_m.

3. *Measurement and Data Plotting*

After the discriminator is calibrated, the modulated signal source is replaced with the frequency source to be measured. Quadrature of the signals into the mixer is reestablished, attenuator No. 4 (Fig. 20) is set to 0 dB, and the measurement process can begin.

The measurements, calculations, and data plotting are completely automated. The calculator program selects the Fourier frequency, performs autoranging, and sets the bandwidth, and measurements of Fourier frequency power are performed by the tracking spectrum analyzer. Each Fourier frequency noise-power reading P_n (dBm) is converted to the corresponding rms voltage by

$$v_{1\,rms} = \sqrt{10^{(P_n + 2.5)/10}/1000 \times R}. \tag{92}$$

The rms frequency fluctuations are calculated as

$$\delta v_{rms} = v_{1\,rms} \times \mathrm{CF}. \tag{93}$$

The spectral density of frequency fluctuations in hertz squared per hertz is calculated as

$$S_{\delta v}(f) = (\delta v_{rms})^2/B, \tag{94}$$

where B is the measured IF noise-power bandwidth of the spectrum analyzer. The spectral density of phase fluctuations in radians squared per hertz is calculated as

$$S_{\delta\phi}(f) = S_{\delta v}(f)/f^2. \tag{95}$$

The NBS-designated spectral density in decibels (carrier) per hertz is calculated as

$$\mathscr{L}(f)_{dB} = 10 \log \tfrac{1}{2} S_{\delta\phi}(f). \tag{96}$$

Spectral density is plotted in real time in our program. However, the data can be stored and the desired spectral density can be plotted in other forms. Integrated phase noise can be obtained as desired.

4. *Noise Floor Measurements*

The relative sensitivity (noise floor) of the single-oscillator measurement system is measured as shown in Fig. 12a for the two-oscillator technique. The delay line must be removed and equal channel lengths constructed, as in Fig. (12a). The same power levels used in the original calibration and measurements are reestablished, and the noise floor is measured at specific Fourier frequencies, using the same calibration–measurement technique, or by repeating the automated measurement sequence.

A correction for the noise floor requires a measurement of the rms voltage of the oscillator ($v_{1\,\mathrm{rms}}$) and a measurement of the noise floor rms voltage ($v_{2\,\mathrm{rms}}$). These voltages are used in the following equation to obtain the corrected value:

$$v_{\mathrm{rms}} = \sqrt{(v_{1\,\mathrm{rms}})^2 - (v_{2\,\mathrm{rms}})^2}. \tag{97}$$

The value v_{rms} is then used in the calculation of frequency fluctuations. If adequate memory is available, each value of $v_{1\,\mathrm{rms}}$ can be stored and used after the other set of measurements are performed at the same Fourier frequencies.

The following technique was developed by Labaar (1982). Carrier suppression is obtained using the rf bridge illustrated in Fig. 18. One can easily improve sensitivity more than 40 dB. At 2.0 and 3.0 GHz 70-dB carrier suppression was realized. In general, the improvement in sensitivity will depend on the availability of an amplifier or adequate input power.

Figure 21 shows the different noise floors in a delay-line bridge discriminator. It is good measurement discipline to always determine these noise floors; also, the measurements, displayed in Fig. 21, give a quick understanding of the physical process involved. The first trace is obtained by terminating the input of the baseband spectrum analyzer. The measured output noise power is then a direct measure of the spectrum analyzer's noise figure (NF). The input noise is thermal noise and is usually indicated by "KTB," which is short for "the thermal noise power at absolute temperature of T degrees K(elvin) per one hertz bandwidth (B). This KTB number is, at 18°C, about −174 dBm/Hz.

Figure 21a shows that trace number 1 for frequencies above about 1 kHz is level with a value of about −150 dBm = −(174–24) dBm, which means that the spectrum analyzer has an NF of 24 dB. At 20 Hz the NF has gone up to about 48 dB. To improve the NF, a low-noise (NF, 2dB), low-frequency (10 Hz–10 MHz) amplifier is inserted as a preamplifier. Terminating its input now results in trace number 2. At the high frequency end, the measured power goes up by about 12–13 dB, and the amplifiers gain is 34 dB. This means that the NF is improved by 34 − 12–13 = 21–22 dB, which is an

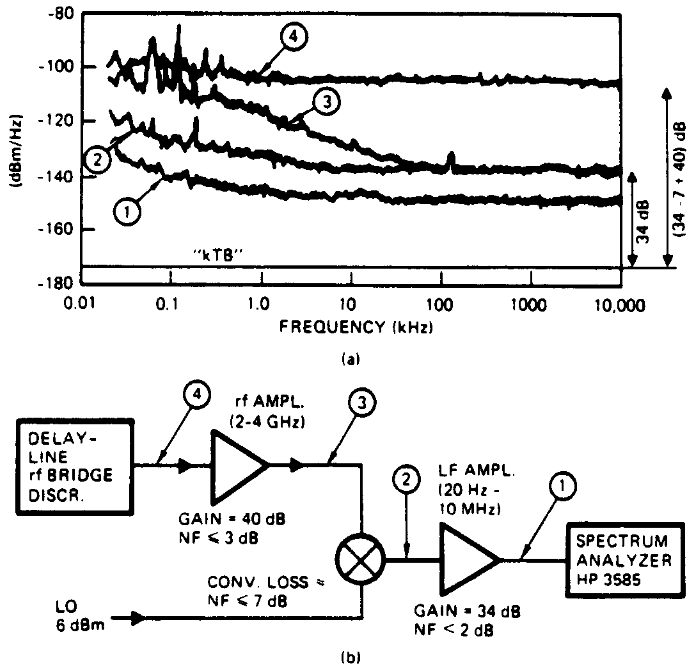

FIG. 21 (a) Noise contribution analysis; (b) phase noise test setup using a delay-line rf bridge discriminator (rf = 2.8 GHz; O, termination points. NF, noise figure; LF, low frequency. (From Seal and Lance, 1981.)

NF $\simeq$ 2–3 dB as expected, i.e., the first stage noise predominates. The low-frequency end at 20 Hz gives an NF of 26 dB, which overall is quite an improvement.

In trace number 3 the mixer is included with it's rf (signal) port terminated. It is clear from this trace that certainly up to 100 kHz, the noise generated by the mixer diodes being "pumped" by the LO signal dominates. This case represents the "classic" delay-line discriminator. The last trace (number 4) includes the low-noise, high-gain rf amplifier that can be used because the carrier is suppressed in the delay-line rf bridge discriminator, in contrast to the classic delay-line discriminator case. This trace shows that from 1 kHz on up the measured output power is flat, representing a 2-3-dB NF.

At about 20–40 Hz, trace numbers 3 and 4 begin nearing their cross-over floor. In this particular case, which is discussed in full by Labaar (1982), the measurement systems noise floor (resolution) has been improved by 40 dB.

Figure 22 shows plots of phase noise as measured at two frequencies using delay lines of different lengths. The delay line used measure at 600 MHz

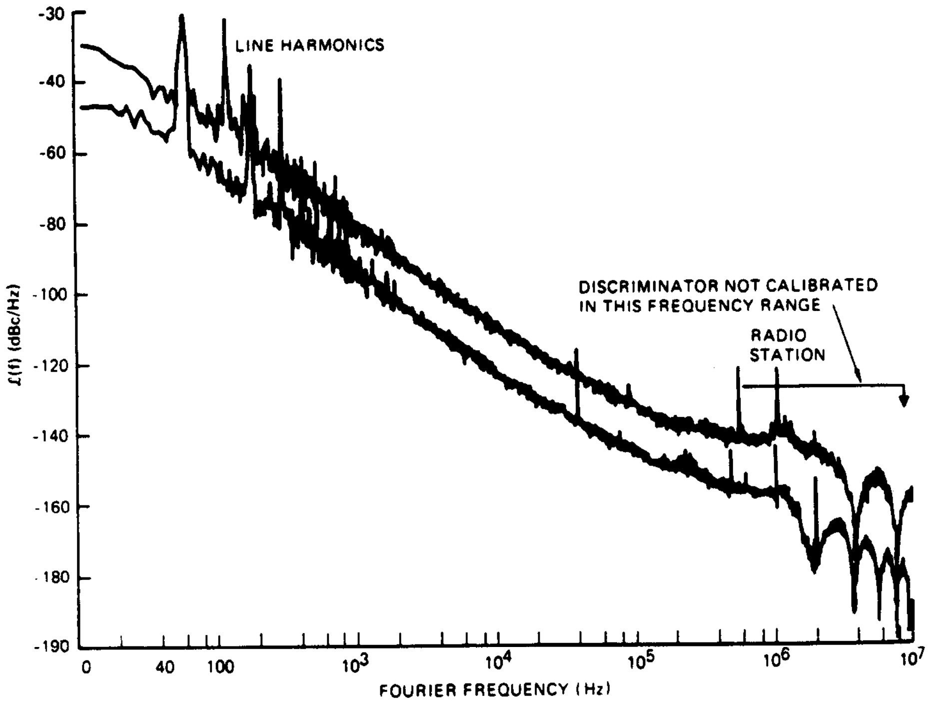

FIG. 22 Phase noise of 600-MHz oscillator multiplied to 2.4 GHz (From Lance *et al.*, 1977a.)

was about 500 nsec long, as noted by the first null, i.e., the reciprocal of the Fourier frequency of 2 MHz is the approximate differential time delay. Note that a shorter delay line (approximately 250 nsec differential) is used to measure the higher frequency because the delay-line discriminator calibration is valid only to a Fourier frequency at approximately 35% of the Fourier frequency at which the first null occurs, if a linear transfer function is assumed.

The actual transfer function of a delay-line discriminator (classic and rf bridge types) is sinusoidal, as shown in Fig. 23a. The baseband spectrum analyzer measures power in a finite bandwidth, and as a consequence it is possible to measure through a transfer-function null if the noise power does not change substantially over a spectrum-analyzer bandwidth. The following power relations then hold:

$$P_{\text{meas}}(\omega) = 1/\Delta\omega \int_{\omega-\Delta\omega/2}^{\omega+\Delta\omega/2} P(\omega')\,d\omega' \simeq \frac{P(\omega)}{\Delta\omega} \int_{\omega-\Delta\omega/2}^{\omega+\Delta\omega/2} d\omega' = P(\omega). \quad (98)$$

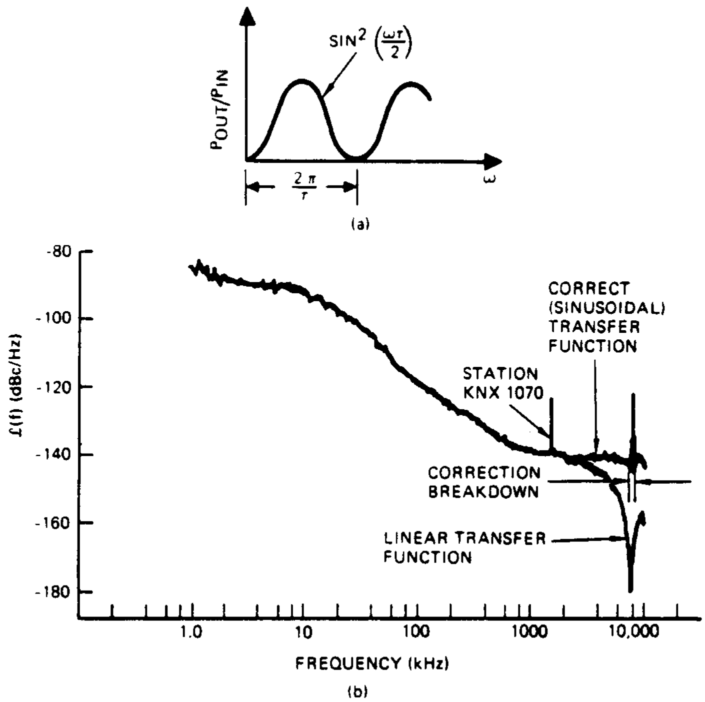

FIG. 23 Transfer functions for a delay-line rf bridge discriminator: (a) actual; (b) approximate (linear) and "correct" (sinusoidal). Phase noise: H.P. 8672A at 2.4 GHz.

Figure 23b shows the results using a linear approximation and the "correct" transfer function for a delay-line rf bridge discriminator. The correct transfer function breaks down close to the null because the signal level drops below the system's noise floor, as explained by Labaar (1982).

Using the sinusoidal transfer function in the calculator software gives correct results barring frequency intervals of 5 to 10 spectrum analyzer's bandwidths (10 × 30 = 300 kHz) centered at the transfer function nulls. These particular data were selected to illustrate the characteristics of the system. Recall that one can easily make the noise floor 40 dB lower using the rf bridge shown in Fig. 18.

C. Dual Delay-Line Discriminator

1. *Phase Noise Measurements*

The dual delay-line discriminator is shown in Fig. 24. This system was suggested by Halford (1975) as a technique for lowering the noise floor of the delay-line phase noise measurement system. The system consists of

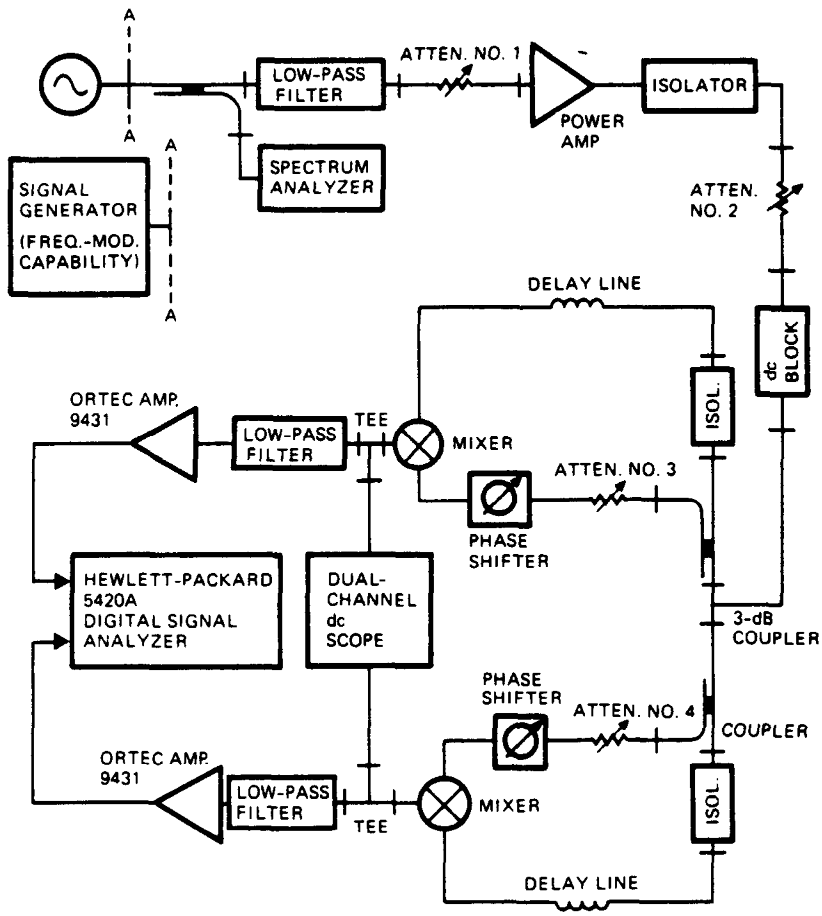

FIG. 24 A dual delay-line phase noise measurement system. (Courtesy Instrument Society of America.)

two differential delay-line systems. The single-oscillator signal is applied to both systems and cross-spectrum analysis is performed on the signal output from the two delay-line systems. Signal processing is performed with the Hewlett-Packard 5420A digital signal analyzer. The *cross spectrum* is obtained by taking the product of the Fourier transform of one signal and the complex conjugate of the Fourier transform of a second signal. It is a phase-sensitive characteristic resulting in a complex product that serves as a measurement of the relative phase of two signals. Cross spectrum gives a phase- and amplitude-sensitive measurement directly. By performing the product $Sy(f) \cdot Sx(f)^*$, a certain signal-to-noise enhancement is achieved.

The low-noise amplifiers preceding the digital signal analyzer are used when performing measurements at Fourier frequencies from 1 Hz to 25 kHz. The amplifiers are not used when performing measurements below the Fourier frequency of 1 Hz.

2. *Calibrating the Dual Delay-Line System*

Each delay line in the system is calibrated separately following the same basic procedure set forth in Section IV.B. The Hewlett-Packard 5420 measures the one-sided spectral density of frequency fluctuations in hertz squared per hertz. The spectral density of phase fluctuation in radians squared per hertz can be calculated as

$$S_{\delta\phi}(f) = S_{\delta v}(f)/f^2, \tag{99}$$

and

$$\mathscr{L}(f) = S_{\delta v}(f)/2f^2, \tag{100}$$

per hertz. The Hewlett-Packard 5420 measurement of $S_{\delta v}(f)$ in Hz^2/Hz must, therefore, be corrected by $1/2f^2$. However, the f^2 correction must be entered in terms of radian frequency ($\omega = 2\pi f$). This conversion is accomplished by

$$\mathscr{L}(f) = S_{\delta v}(f)(1/2f^2)(4\pi^2/4\pi^2) = [2\pi^2 S_{\delta v}(f)]/(\omega)^2 \tag{101}$$

per hertz since Eq. (100) can be stated in the following terms:

$$[2\pi^2 S_{\delta v}(f)]/4\pi^2 f^2.$$

Signal-to-noise enhancement greater than 20 dB has been obtained using the dual-channel delay-line system.

D. Millimeter-Wave Phase-Noise Measurements

1. *Spectral Density of Phase Fluctuations*

The delay line used as an FM discriminator is based, in principle, on a *nondispersive* delay line. However, a waveguide can be used as the delay line because the Fourier frequency range of interest is a small percentage of the operating bandwidth (seldom over 100 MHz), and the dispersion can be considered negligible.

The calibration and measurement are performed as set forth in Section IV.B. The modulation index m is usually established using the carrier-to-sideband ratio that uses amplitude modulation because millimeter sources are either unstable or cannot be modulated. The two approaches to measurements at millimeter frequencies are shown in Figs. 25 and 26. Figure 25 shows the *direct measurement* using a waveguide delay line. This system offers improved sensitivity if adequate input power is available. The rf bridge and delay-line portion of the system differs from Fig. 18 because pre- and

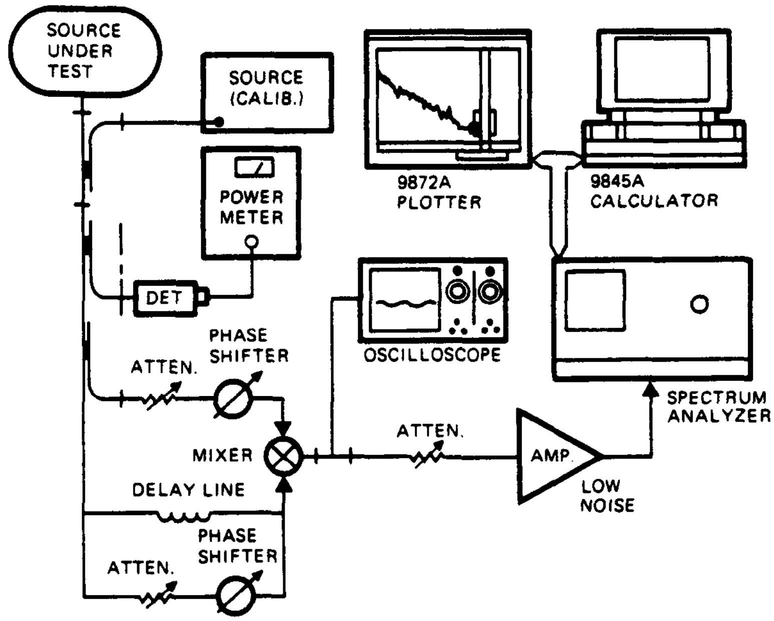

FIG. 25 Millimeter-wave phase noise measurements using a waveguide delay line. (From Seal and Lance, 1981.)

post-bridge amplifiers with appropriate gain are not available, so the sensitivity can equal the amount of carrier suppression.

Figure 26 shows the use of a harmonic mixer to downconvert to the convenient lower frequency where post-bridge amplifiers are available. The relatively low sensitivity to frequency drift that is characteristic of delay-line discriminators becomes an advantage here. A separate calibration generator is required, as shown in Fig. 25, and a power meter is used to assure proper power levels during the calibration process.

2. SPECTRAL DENSITY OF AMPLITUDE FLUCTUATIONS

AM noise measurements require equal electrical length in the two channels that supply the signals to the mixer. The delay line must be replaced with the necessary length of transmission line to establish the equal-length condition when the systems shown in Figs. 25 and 26 are used. The AM noise measurement system is calibrated and the noise measurements are performed directly in units of power for a direct measurement of $m(f)$ in dBc/Hz. $m(f)$ is the spectral density of one modulation sideband divided by the total signal power at a Fourier frequency difference f from the signal's average frequency ν_0. The system calibration establishes the detection characteristics in terms of total power output at the IF port of the mixer (detector).

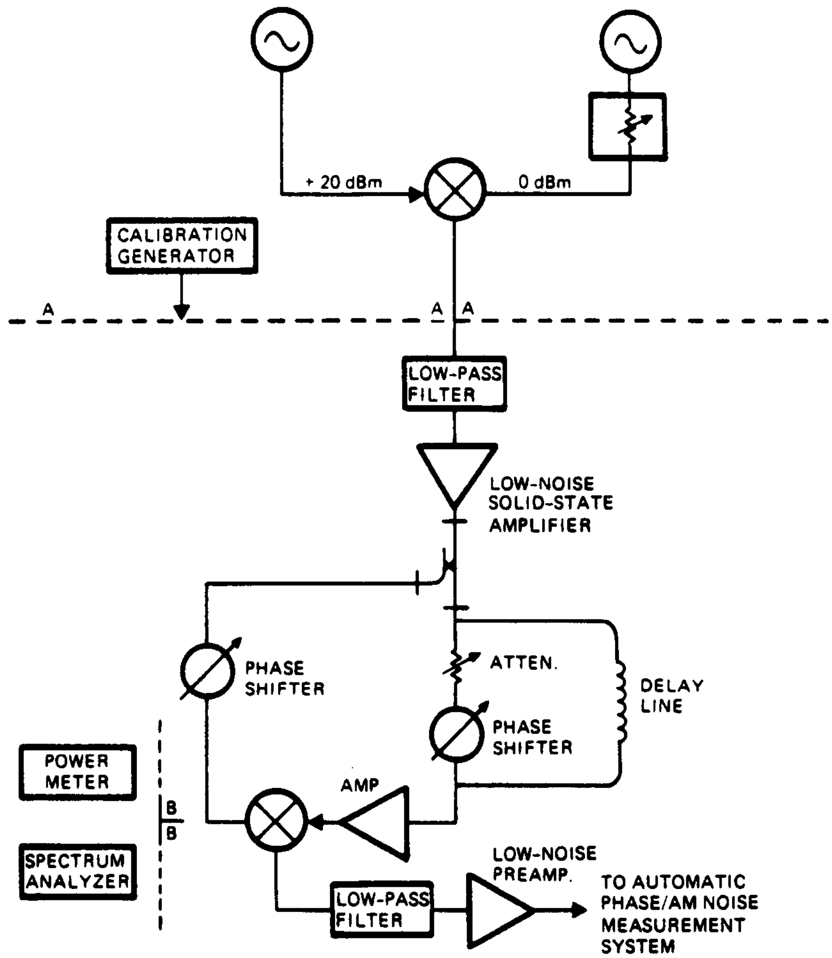

FIG. 26 A millimeter-wave hybrid phase noise measurement system that produces IF frequency and uses a delay-line discriminator at IF frequency. (From Seal and Lance, 1981.)

The AM noise measurements are performed according to the following.

(1) A known AM modulation (carrier-sideband ratio) must be established to calibrate this detector in terms of total power output at the IF port. The modulation must be low enough so that the sidebands are at least 20 dB below the carrier. This is to keep the total added power due to the modulation small enough to cause an insignificant change in the detector characteristics.

(2) The rf power levels are adjusted for levels of approximately 10 dBm at the reference port and 0 dBm at the test port of the mixer.

(3) Approximately 40 dB is set in the precision IF attenuator. The system is adjusted for an *out-of-phase quadrature condition.*

(4) The modulation frequency and power level are measured by the automatic baseband spectrum analyzer. The total carrier-power reference level is measured power, plus the carrier–sideband modulation ratio, plus the IF attenuator setting.

(5) The AM modulation is removed. the IF attenuator set to 0 dB, and the system re-checked to verify the out-of-phase quadrature (maximum dc output from the mixer IF port). Noise (V_n) is measured at the selected Fourier frequencies. A direct calculation of $m(f)$ in dBc/Hz is

$$m(f) = [(\text{modulation power (dBm)} + \text{carrier–sideband ratio (dB)} + \text{IF attenuation (dB)} - \text{noise power (dBm)} + 2.5\ \text{dB} - 10\log(\text{BW})]. \tag{102}$$

Figure 27 illustrates the measurements of AM and phase noise of two GUNN oscillators that were offset in frequency by 1 GHz. The measurements were performed using the coaxial delay-line system.

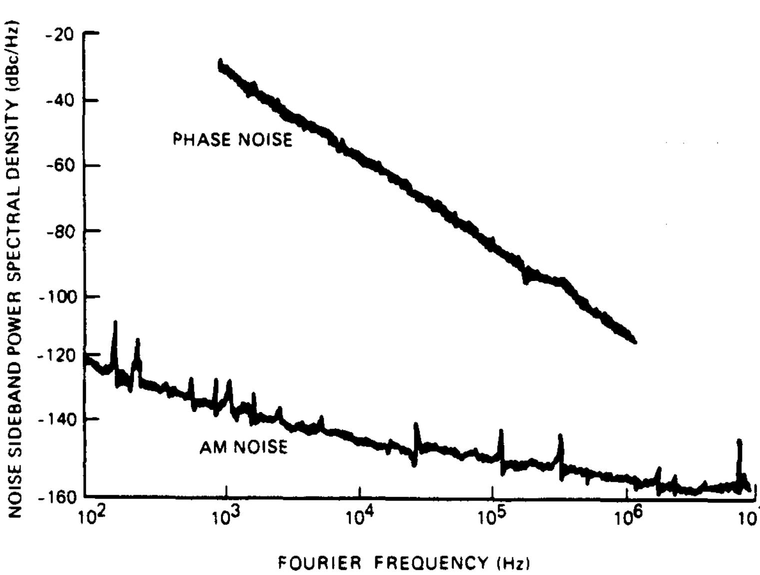

FIG. 27 Phase noise and AM noise of 40- and 41-GHz Gunn oscillators. (From Seal and Lance, 1981.)

V. Conclusion

The fundamentals and techniques for measurement of phase noise have been set forth for two basic systems. The two-oscillator technique provides the capability for measuring high-performance cw sources. The system sensitivity is superior to the single-oscillator technique for measuring phase noise very close to the carrier.

High-stability sources such as those used in frequency standards applications can be measured without using phase-locked loops. However, most microwave sources exhibit frequency instability that requires phase-locked loops to maintain the necessary quadrature conditions. The characteristics of the phase-locked loops must be evaluated to obtain the source phase noise characteristics. Also, in principle, one must have three sources at the same frequency to characterize a given source. If three sources are not available, one must assume that either one source is superior in performance or that they have equal phase noise contributions.

The single-oscillator technique employing the delay line as an FM discriminator has adequate sensitivity for measuring most microwave sources. The economic advantages of using this system include the fact that only one source is required, phase-locked loops are not required, system configuration is relatively inexpensive, and the system is inherently insensitive to oscillator frequency drift.

The single-oscillator technique using the delay-line discriminator can be adapted to measure the phase noise of pulsed sources. Pulsed sources have been measured at 94 GHz by F. Labaar at TRW, Redondo Beach, California.

Acknowledgments

Our initial preparations for developing a phase noise measurement capability were the result of discussions with Dr. Jorg Raue of TRW. Our first phase noise development effort was assisting in the evaluation of phase noise measurement systems designed and developed by Bill Hook of TRW (Hook, 1973). The efforts of Don Leavitt of TRW were vital in initiating the measurement program.

We are very grateful to Dr. Donald Halford of the National Bureau of Standards in Boulder, Colorado, for his interest, consultations, and valuable suggestions during the development of the phase noise measurement systems at TRW.

We appreciate the measurement cross-checks performed by C. Reynolds, J. Oliverio, and H. Cole of the Hewlett-Packard Company, Dr. J. Robert Ashley of the University of Colorado, Colorado Springs, and G. Rast of the U.S. Army Missile Command, Redstone Arsenal, Huntsville, Alabama.

References

Allen, D. W. (1966). *Proc. IEEE* **54**, 221–230.

Ashley, J. R., Searles, C. B., and Palka, F. M. (1968). *IEEE Trans. Microwave Theory Tech.* MTT-16(9), 753–760.

Ashley, J. R., Barley, T. A., and Rast, G. J. (1977). *IEEE Trans. Microwave Theory Tech.* **MTT-25**(4), 294–318.

Baghdady, E. J., Lincoln, R. N., and Nelin, B. D. (1965). *Proc. IEEE* **53**, 704–722.

Barnes, J. A. (1969). "Tables of Bias Functions, B_1 and B_2, for Variances Based on Finite Samples of Processes with Power Law Spectral Densities," National Bureau of Standards Technical Note 375.

Barnes, J. A., Chie, A. R., and Cutler, L. S. (1970). "Characterization of Frequency Stability," National Bureau of Standards Technical Note 394; also published in *IEEE Trans. Instrum. Meas.* **IM-20**(2), 105–120 (1971).

Brandenberger, H., Hadorn, F., Halford, D., and Shoaf, J. H. (1971). *Proc. 25th Ann. Symp. Freq. Control*, Fort Monmouth, New Jersey, pp. 226–230.

Culter, L. S., and Searle, C. L. (1966). *Proc. IEEE* **54**, 136–154.

Fisher, M. C. (1978). "Frequency Domain Measurement Systems," Paper presented at the 10th Annual Precise Time and Time Interval Applications and Planning Meeting, Goddard Space Flight Center, Greenbelt, Maryland. *

Halford, D. (1968). *Proc. IEEE* **56**(2), 251–258.

Halford, D. (1975). "The Delay Line Discriminator," National Bureau of Standards Technical Note 10, pp. 19–38.

Halford, D., Wainwright, A. E., and Barnes, J. A. (1968). *Proc. 22nd Ann. Symp. Freq. Control*, Fort Monmouth, New Jersey, 340–341.

Halford, D., Shoaf, J. H., and Risley, A. S. (1973). *Proc. 27th Ann. Symp. Freq. Control*, Cherry Hill, New Jersey, pp. 421–430.

Hook, W. R. (1973). "Phase Noise Measurement Techniques for Sources Having Extremely Low Phase Noise," TRW Defense and Space Systems Group Internal Document, Redondo Beach, California.

Hewlett-Packard Company (1965). "Frequency and Time Standards," Application Note 52. Hewlett-Packard Co., Palo Alto, California.

Hewlett-Packard Company (1970). "Computing Counter Applications Library," Application Notes 7, 22, 27, and 29. Hewlett-Packard Co., Palo Alto, California.

Hewlett-Packard Company (1976). "Understanding and Measuring Phase Noise in the Frequency Domain," Application Note 207. Hewlett-Packard Co., Loveland, Colorado.

Labaar, F. (1982). "New Discriminator Boosts Phase Noise Testing." *Microwaves* **21**(3), 65–69.

Lance, A. L. (1964). "Introduction to Microwave Theory and Measurements." McGraw-Hill, New York.

Lance, A. L., Seal, W. D., Mendoza, F. G., and Hudson, N. W. (1977a). *Microwave J.* **20**(6), 87–103.

Lance, A. L., Seal, W. D., Mendoza, F. G., and Hudson, N. W. (1977b). *Proc. 31st Annu. Symp. Freq. Control*, Atlantic City, New Jersey, pp. 463–483.

Lance, A. L., Seal, W. D., Halford, D., Hudson, N., and Mendoza, F. (1978). "Phase Noise Measurements Using Cross-Spectrum Analysis." Paper presented at the IEEE Conference on Electromagnetic Measurements, Ottawa, Canada.

Lance, A. L., Seal, W. D., and Labaar, F. (1982). *ISA Trans.* **21**(4), 37–44.

Meyer, D. G. (1970). *IEEE Trans.* **IM-19**(4), 215–227.

Ondria, J. (1968). *IEEE Trans. Microwave Theory Tech.* **MTT-16**(9), 767–781.

Ondria, J. G. (1980). *IEEE-MTT-S Int. Microwave Symp. Dig.*, pp. 24–25.

Payne, J. B., III (1976). *Microwave System News* **6**(2), 118–128.

Scherer, D. (1979). "Design Principles and Measurement Low Phase Noise RF and Microwave Sources." Hewlett-Packard Co., Palo Alto, California.

Seal, W. D., and Lance, A. L. (1981). *Microwave System News* **11**(7), 54–61.

Shoaf, J. H., Halford, D., and Risley, A. S. (1973). "Frequency Stability Specifications and Measurement." National Bureau of Standards Technical Note 632.

* See Appendix Note # 33

Tykulsky, A. (1966). *Proc. IEEE* **54**(2), 306.
Van Duzer, V. (1965). *Proc. IEEE-NASA Symp. Definition Meas. Short-Term Freq. Stability*, NASA SP-80, 269–272.
Walls, F. L., and Stein, S. R. (1977). *Proc. 31st Ann. Symp. Freq. Control*, Atlantic City, New Jersey, pp. 335–343.
Walls, F. L., Stein, S. R., Gray, J. E., Glaze, D. J., and Allen, D. W. (1976). *Proc. 30th Ann. Symp. Freq. Control*, Atlantic City, New Jersey, p. 269.